Journal of Medicinal Chemistry

Article

pubs.acs.org/jmc

Design, Synthesis, and Pharmacological Characterization of *N*- and *O*-Substituted 5,6,7,8-Tetrahydro-4*H*-isoxazolo[4,5-*d*]azepin-3-ol Analogues: Novel 5-HT_{2A}/5-HT_{2C} Receptor Agonists with Pro-Cognitive Properties

Anders A. Jensen,*[,†] Niels Plath,[‡] Martin H. F. Pedersen,[§] Vignir Isberg,[†] Jacob Krall,[†] Petrine Wellendorph,[†,∥] Tine B. Stensbøl,[‡] David E. Gloriam,[†] Povl Krogsgaard-Larsen,[†] and Bente Frølund[†]

[†]Department of Drug Design and Pharmacology, Faculty of Health and Medical Sciences, University of Copenhagen, Universitetsparken 2, Copenhagen, Denmark

[‡]H. Lundbeck A/S, Valby, Denmark

[§]Hevesy Laboratory, Radiation Research Division, Risø, Technical University of Denmark, Roskilde, Denmark

[∥]Neurobiology Research Unit and Center for Integrated Molecular Brain Imaging (Cimbi), Rigshospitalet and University of Copenhagen, Copenhagen, Denmark

Supporting Information

ABSTRACT: The isoxazol-3-one tautomer of the bicyclic isoxazole, 5,6,7,8-tetrahydro-4*H*-isoxazolo-[4,5-*d*]azepin-3-ol (THAZ), has previously been shown to be a weak $GABA_A$ and glycine receptor antagonist. In the present study, the potential in this scaffold has been explored through the synthesis and pharmacological characterization of a series of *N*- and *O*-substituted THAZ analogues. The analogues *N*-Bn-THAZ (**3d**) and *O*-Bn-THAZ (**4d**) were found to be potent agonists of the human 5-HT_{2A} and 5-HT_{2C} receptors. Judging from an elaborate pharmacological profiling at numerous other CNS targets, the **3d** analogue appears to be selective for the two receptors. Administration of **3d** substantially improved the cognitive performance of mice in a place recognition Y-maze model, an effect fully reversible by coadministration of the selective 5-HT_{2C} antagonist SB242084. In conclusion, as novel bioavailable cognitive enhancers that most likely mediate their effects through 5-HT_{2A} and/or 5-HT_{2C} receptors, the isoxazoles **3d** and **4d** constitute interesting leads for further medicinal chemistry development.

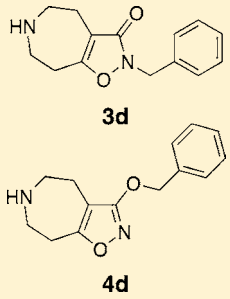

INTRODUCTION

The neurotransmitter serotonin (5-hydroxytryptamine, 5-HT) is widely distributed throughout the central nervous system (CNS) and the peripheral nervous system.[1] In the periphery, 5-HT regulates a broad spectrum of functions in the cardiovascular, gastrointestinal, endocrine, pulmonary, and genitourinary systems.[1−4] In the CNS, 5-HT plays key roles in processes involved in mood, libido, aggression, anxiety, cognition, sleep, appetite sensation, as well as pain perception and processing. During the last five decades, serotonergic ligands have proven effective drugs in the treatment of migraine, pain, obesity, and a wide range of psychiatric and neurological disorders, and intervention in central serotonergic neurotransmission continues to be intensively pursued in the search for new therapeutics against these indications.[1,5−9]

5-HT mediates its physiological effects through six classes of 7-transmembrane (7-TM) receptors (5-HT_1, 5-HT_2, 5-HT_4, 5-HT_5, 5-HT_6, and 5-HT_7) containing a total of 13 subtypes[10−12] and through a class of cation-selective ligand-gated ion channels, the 5-HT_3 receptors.[13] This heterogeneity is further increased by the fact that several of the receptors are subjected to splice variation or RNA editing.[10−12] The 5-HT_2 receptor class consists of the 5-HT_{2A}, 5-HT_{2B}, and 5-HT_{2C} subtypes, which are $G_{q/11}$-protein coupled receptors functionally linked to activation of phospholipase C and the resulting formation of the second messengers 1,4,5-trisphosphate and diacylglycerol and mobilization of intracellular calcium, as well as to other intracellular signaling cascades.[14,15] The 5-HT_{2A} subtype is heterogeneously expressed in the CNS, and the receptor constitutes a major drug target in psychiatric diseases and is believed to be the main mediator of the psychotropic and psychotomimetic effects of natural product compounds like lysergic acid diethylamide (LSD) and psilocybin as well as several synthetic drugs.[1,16,17] The 5-HT_{2B} receptor is widely expressed in the periphery, where it for example is involved in regulation of gastrointestinal motility and bone metabolism, and the receptor has been linked with vascular pathologies such as cardiac hypertrophy and pulmonary hypertension.[18,19] Finally, the 5-HT_{2C} receptor is almost exclusively found in the CNS where it is even more abundantly expressed than 5-HT_{2A}. 5-HT_{2C} receptors are predominantly found postsynaptically to serotonergic terminals, where they act

Received: November 9, 2012
Published: January 9, 2013

as somatodendritic heteroreceptors on glutamatergic, dopaminergic, and GABAergic neurons and interneurons in several regions.[14,15,20−22] These modulatory role held by the receptor for the activities in these three neurotransmitter systems have prompted investigations of 5-HT$_{2C}$ receptors as putative targets for the treatment of a wide range of neurological and psychiatric disorders.[22−26]

In the present study, we report the discovery of a novel class of subtype-selective and potent 5-HT receptor agonists based on the 5,6,7,8-tetrahydro-4*H*-isoxazolo[4,5-*d*]azepin-3-ol (THAZ) scaffold (Figure 1). THAZ is a seven-membered ring analogue of

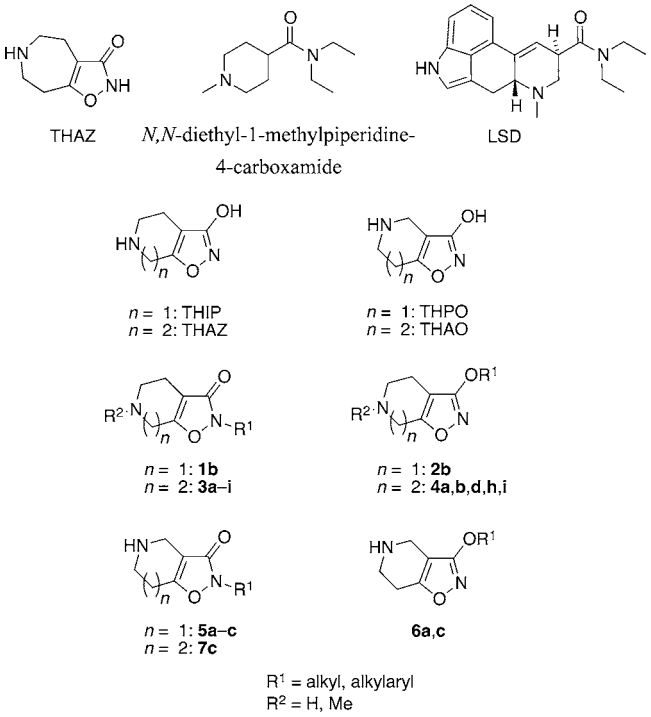

Figure 1. Chemical structures of the THIP, THAZ, THPO, and THAO analogues investigated in this study.

the γ-aminobutyric acid type A (GABA$_A$) receptor agonist 4,5,6,7-tetrahydroisoxazolo[5,4-*c*]pyridin-3-ol (THIP)[27] (Figure 1), and in previous studies THAZ has been shown to be a weak antagonist of native glycine and GABA$_A$ receptors.[28−30] Our interest in the THAZ scaffold in the present study arose from its structural similarity as the isoxazole-3-one tautomer to the 5-HT receptor agonist *N*,*N*-diethyl-1-methylpiperidine-4-carboxamide[31] and the tetrahydropyridine carboxamide part of LSD (Figure 1). We have synthesized a series of *N*- and *O*-substituted THAZ analogues and identified a couple of relatively potent agonists of the 5-HT$_{2A}$ and 5-HT$_{2C}$ receptors. One of these, *N*-Bn-THAZ (**3d**), is shown to be a selective 5-HT$_{2A}$/5-HT$_{2C}$ agonist displaying negligible activity at other 5-HT receptors and at a plethora of other CNS targets. In the search for other putative CNS targets for **3d** the binding distribution of an ^{125}I-labeled analogue of the compound in rat brain tissue has been mapped, and the therapeutic potential in **3d** has been investigated in animal tests for cognitive function and schizophrenia.

RESULTS

Chemistry. The synthesis of the THAZ, THIP, 4,5,6,7-tetrahydroisoxazolo[4,5-*c*]pyridin-3-ol (THPO), and 5,6,7,8-tetrahydro-4*H*-isoxazolo[4,5-*c*]azepin-3-ol (THAO) analogues (**1b**, **2b**, **3a−i**, **4a,b,d,i**, **5a−c**, **6a,c**, **7c**) is illustrated in Schemes 1 and 2 and follow similar strategy. *N*-Methoxycarbonyl protected THIP (**8**),[32] THAZ (**9**),[28] THPO (**14**),[32] and THAO (**15**)[28] were alkylated using the approriate alkyl or alkylaryl halide in the presence of potassium carbonate. The alkylation step gave rise to a mixture of the *N*-alkylated (**10b**, **12a−g**, **16a−c**) and *O*-alkylated (**11b**, **13a−g**, **17a−c**) isomers, which were separated using column chromatography. Deprotection was performed using acidic or basic conditions. Reductive amination using aqueous formic acid and formaldehyde led to the *N*-methylated analogues **3h,i** and **4h,i**.

Scheme 1[a]

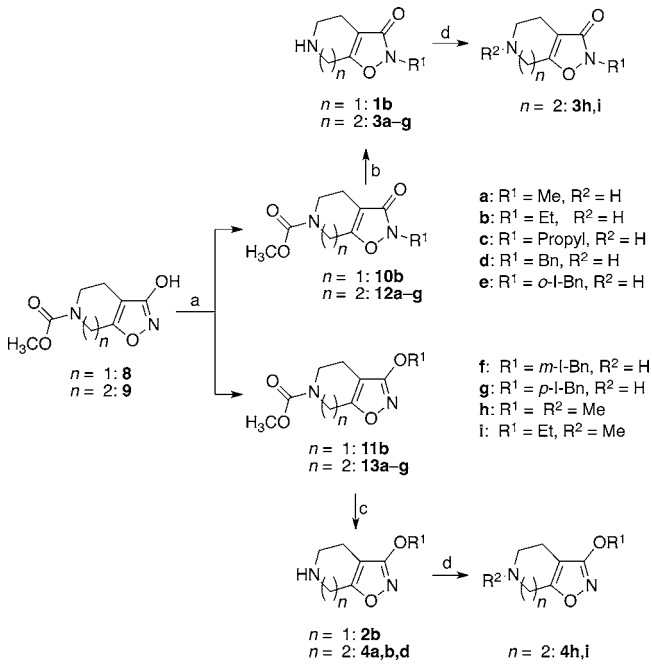

[a]Reagents and conditions: (a) K_2CO_3, R^{1}X, acetone; (b) 33% HBr/AcOH; (c) KOH/MeOH; (d) aq HCO_2H, HCHO.

Scheme 2[a]

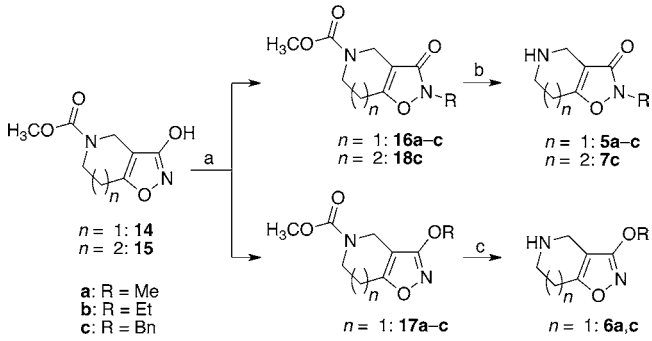

[a]Reagents and conditions: (a) K_2CO_3, R^{1}X, acetone; (b) 33% HBr/AcOH or HCl/AcOEt; (c) KOH/MeOH.

The synthesis of the stannyl precusor for the radioligand [^{125}I] *N*-Bn-THAZ) (**21**), was performed using the *N*-protected *p*-I-Bn-THAZ analogue (**12g**), synthesized as described (Scheme 3). Compound **12g** was treated with hexabutyldistannane in the

dx.doi.org/10.1021/jm301656h | J. Med. Chem. 2013, 56, 1211−1227

Scheme 3[a]

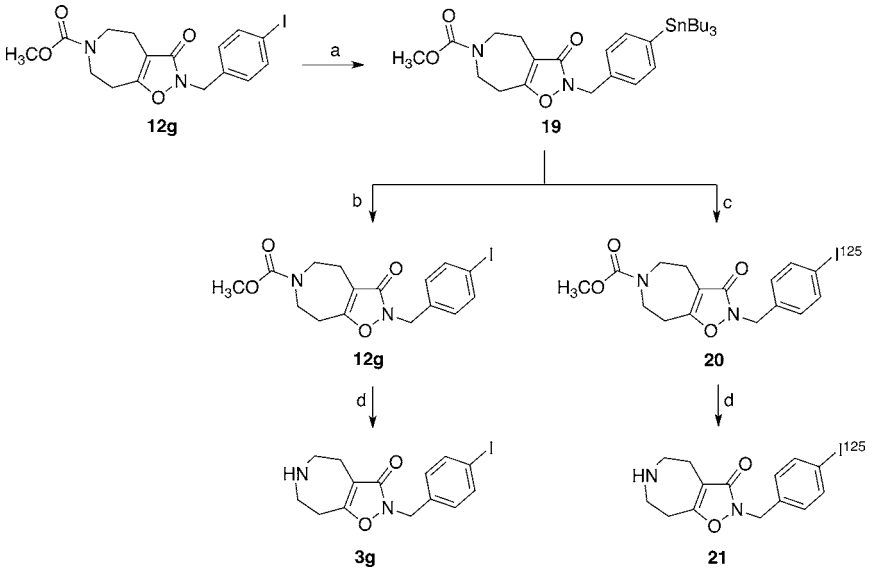

[a]Reagents and conditions: (a) $Pd(PPh_3)_4$, $(SnBu_3)_2$, toluene, reflux 22 h; (b) NaI, chloramine-T in a mixture of 94% EtOAc, 4% DMF, 1% AcOH, 1% H_2O, room temp, 30 min, $Na_2S_3O_5$; (c) 44.0 MBq $Na^{125}I$, chloramine-T in a mixture of 94% EtOAc, 4% DMF, 1% AcOH, 1% H_2O, room temperature, 30 min; (d) 33% HBr/AcOH, room temperature 5 h.

presence of tetrakis(triphenylphosphine)Pd(0) in refluxing toluene to furnish the stannylated derivative **19**. To test the efficiency of the iodination reaction, **19** was initially converted into the cold ligand **12g** by reaction with NaI under oxidative conditions with chloramine-T in a mixture of ethyl acetate, dimethylformamide, acetic acid, and water, followed by deprotection with hydrobromide in acetic acid. As this strategy proved functional, the radioligand was generated in a similar fashion. Thus, radioiodination was carried out by treatment with $Na^{125}I$ using the chloramine-T method followed by deprotection with hydrobromide in acetic acid. The radioligand **21** was purified by HPLC and analyzed to have a radiochemical purity of 100% and a total activity of 40.3 MBq (yield: 91% based on $Na^{125}I$).

Functional Characterization of THAZ, THIP, THPO, and THAO Analogues at 5-HT$_{2A}$ and 5-HT$_{2C}$ in the Fluo-4/Ca^{2+} Assay. Preliminary testing suggested that some of the synthesized THAZ analogues possessed agonist activity at 5-HT_2 receptors (data not shown). To characterize the functional properties of the compounds in greater detail, two polyclonal HEK293 cell lines stably expressing the human 5-HT_{2A} and 5-HT_{2C} receptors were constructed. To validate the pharmacological properties exhibited by the receptors expressed in these cells, 10 reference 5-HT_2 receptor ligands were characterized functionally at the cell lines in the fluorescence-based Fluo-4/Ca^{2+} assay that measures the release of Ca^{2+} from intracellular stores upon activation of the $G_{q/11}$-coupled receptors.[14,15] The rank orders of agonist potencies and to some extent also the absolute EC_{50} values displayed by 5-HT, PNU-22394, Ro 60-0175, CP 809101, MK-212, and WAY 161503 at the receptors in this assay were in good agreement with findings from previous studies (Table 1 and Figure 2A).[33−36] Also, in concordance with previous studies, the five selective 5-HT_2 agonists were found to be full agonists or high-efficacy partial agonists at both subtypes, displaying maximal responses similar to or slightly lower than those of 5-HT at the two receptors.[33,34,36−38] The K_i values obtained for four reference 5-HT_2 receptor antagonists at the receptors also correlated well with those obtained in previous studies.[33,38−42] Both mianserin and asenapine were found to be equipotent antagonists at 5-HT_{2A} and 5-HT_{2C}, clozapine displayed a preference (~8-fold) for 5-HT_{2A} over 5-HT_{2C}, and MDL 11,939 was a highly selective 5-HT_{2A} antagonist exhibiting a ~4000-fold lower K_i at this receptor than at 5-HT_{2C} (Table 1). All agonists and antagonists displayed Hill slopes close to unity ($n_H \sim 1$) at the two receptors (data not shown).

When characterized in the Fluo-4/Ca^{2+} assay the majority of the 12 THAZ analogues (THAZ, **3a−d**, **3h−i**, **4a−b**, **4d**, **4h−i**) were found either to be weak agonists at the 5-HT_{2A} and 5-HT_{2C} receptors or to be completely inactive as agonists and antagonists at concentrations up to 1 mM (Table 1 and Figure 2A). However, notable exceptions were the *N*- and *O*-benzylated THAZ analogues **3d** and **4d**, which were potent agonists displaying high nanomolar EC_{50} values at both receptors. Whereas **3d** was a high-efficacious partial agonist at both subtypes, **4d** was a pronounced partial agonist at 5-HT_{2A}, eliciting a maximal response of 59% of that of 5-HT at the receptor (Table 1 and Figure 2A). The 5-HT_{2A} and 5-HT_{2C} activity of the THAZ analogues prompted us to test series of *N*- and *O*-substituted analogues of the structurally related scaffolds THIP, THPO, and THAO at the receptors. However, none of these compounds (**1b**, **2b**, **5a−c**, **6a**, **6c**, **7c**) displayed substantial pharmacological activity at the receptors (Table 1).

*Functional Characterization of THAZ Analogues **3d** and **4d** at 5-HT$_{2A}$ and 5-HT$_{2C}$ in the IP-One Assay.* The agonist activity displayed by **3d** and **4d** at the 5-HT_{2A} and 5-HT_{2C} receptors in the Fluo-4/Ca^{2+} assay was verified in the IP-One assay, in which the formation and accumulation of the second messenger inositol monophosphate (IP_1) upon activation of the receptors is measured.[43] The agonist potencies displayed by **3d** and **4d** in the IP-One assay were slightly lower (2−5-fold) than those exhibited by the agonists in the Fluo-4/Ca^{2+} assay (Tables 1 and 2). However, the same was true for the reference agonists CP 809101 and MK-212 and even more pronounced differences in agonist potencies between the two assays were observed for 5-HT and PNU 22394 (Tables 1 and 2). The rank orders of potencies displayed by the six agonists at 5-HT_{2A} were 5-HT >

dx.doi.org/10.1021/jm301656h | J. Med. Chem. 2013, 56, 1211−1227

Table 1. Functional Properties of Reference Ligands and THAZ, THIP, THPO, and THAO Analogues at Polyclonal h5-HT$_{2A}$-HEK293 and h5-HT$_{2C}$-HEK293 Cell Lines in the Fluo-4/Ca^{2+} Assay[a]

	h5-HT$_{2A}$		h5-HT$_{2C}$	
	EC$_{50}$ [pEC$_{50}$ ± SEM]	R_{max} ± SEM	EC$_{50}$ [pEC$_{50}$ ± SEM]	R_{max} ± SEM
5-HT	0.0026 [8.59 ± 0.06]	*100*	0.00087 [9.06 ± 0.08]	*100*
PNU 22394	0.023 [7.63 ± 0.12]	*102 ± 9*	0.0077 [8.11 ± 0.13]	*101 ± 5*
Ro 60−0175	0.027 [7.57 ± 0.10]	*117 ± 12*	0.0047 [8.33 ± 0.13]	*111 ± 10*
CP 809101	0.076 [7.12 ± 0.17]	*88 ± 6*	0.0019 [8.72 ± 0.18]	*103 ± 8*
MK-212	0.42 [6.37 ± 0.04]	*97 ± 7*	0.028 [7.55 ± 0.11]	*93 ± 8*
WAY 161503	0.012 [7.93 ± 0.05]	*110 ± 12*	0.0073 [8.13 ± 0.12]	*95 ± 10*
	K_i [pK_i ± SEM]		K_i [pK_i ± SEM]	
mianserin	0.0081 [8.09 ± 0.13]		0.0080 [8.09 ± 0.14]	
clozapine	0.0091 [8.04 ± 0.09]		0.073 [7.14 ± 0.15]	
asenapine	0.00091 [9.04 ± 0.17]		0.0025 [8.61 ± 0.09]	
MDL 11,939	0.0025 [8.61 ± 0.09]		∼10 [∼5.0]	
	EC$_{50}$ [pEC$_{50}$ ± SEM]	R_{max} ± SEM	EC$_{50}$ [pEC$_{50}$ ± SEM]	R_{max} ± SEM
THAZ analogues				
THAZ	>1000 [<3.0][b]		>1000 [<3.0][b]	
3a	weak agonist[c]		weak agonist[c]	
3b	agonist[d]		agonist[d]	
3c	agonist[d]		agonist[d]	
3d	0.55 [6.26 ± 0.04]	*80 ± 6.5*	0.42 [6.38 ± 0.08]	*90 ± 5.6*
3h	>1000 [<3.0][b]		>1000 [<3.0][b]	
3i	>1000 [<3.0][b]		>1000 [<3.0][b]	
4a	agonist[d]		12 [4.92 ± 0.08]	*80 ± 4.1*
4b	7.9 [5.10 ± 0.08]	*42 ± 3.1*	3.0 [5.53 ± 0.12]	*67 ± 5.6*
4d	0.24 [6.61 ± 0.10]	*59 ± 5.8*	0.10 [6.99 ± 0.13]	*84 ± 2.7*
4h	>1000 [<3.0][b]		weak agonist[c]	
4i	>1000 [<3.0][b]		>1000 [<3.0][b]	
THIP analogues				
1b	>1000 [<3.0][b]		>1000 [<3.0][b]	
2b	>1000 [<3.0][b]		>1000 [<3.0][b]	
THPO analogues				
5a	>1000 [<3.0][b]		>1000 [<3.0][b]	
5b	>1000 [<3.0][b]		>1000 [<3.0][b]	
5c	>1000 [<3.0][b]		>1000 [<3.0][b]	
6a	agonist[d]		agonist[d]	
6c	weak agonist[c]		weak agonist[c]	
THAO analogue				
7c	>1000 [<3.0][b]		>1000 [<3.0][b]	

[a]The EC$_{50}$ values are given in μM with pEC$_{50}$ ± SEM values in brackets, and R_{max} ± SEM values are given in % of the R_{max} obtained for 5-HT at the same receptor at the same plate. In the antagonist experiments, EC$_{75}$−EC$_{85}$ concentrations of 5-HT were used. Data are the means of 4−10 individual experiments performed in duplicate. [b]No significant agonist or antagonist activity at 1 mM. [c]Weak agonist response at concentrations of 100−1000 μM. [d]The concentration−response curve of the agonist was not complete at concentrations up to 1000 μM.

PNU 22394 > CP 809101 > **4d** > MK-212 ∼ **3d** in the Fluo-4/Ca^{2+} assay and CP 809101−5-HT ∼ PNU 22394 > MK-212 ∼ **4d** > **3d** in IP-One assay. At the 5-HT$_{2C}$ receptor, the potency rank orders were 5-HT > CP 809101 > PNU 22394 > MK-212 > **4d** > **3d** in the Fluo-4/Ca^{2+} assay and CP 809101 > 5-HT > PNU 22394 ∼ MK-212 ∼ **4d** > **3d** in the IP-One assay. Thus, the rank orders of agonist potencies at the two receptors were fairly similar in the two assays, the major difference being the relatively higher potencies of CP 809101 in the IP-One assay compared to the Fluo-4/Ca^{2+} assay. The differences between the absolute EC$_{50}$ values measured for the agonists are thus likely to arise from the inherent differences between the two assays, the one measuring transient increases in intracellular Ca^{2+} concentrations and the other accumulation of IP$_1$ in the cells over a longer period of time (see Experimental Section). In agreement with its profile in the Fluo-4/Ca^{2+} assay, **4d** displayed partial agonism at 5-HT$_{2A}$ in the IP-One assay, whereas the maximal responses elicited by **4d** at 5-HT$_{2C}$ and by **3d** at both 5-HT$_{2A}$ and 5-HT$_{2C}$ were not significantly different from those of 5-HT at the respective receptors (Figure 2B and Table 2).

Binding Properties of the THAZ Analogues at the 5-HT$_{2A}$ and 5-HT$_{2C}$ Receptors. The binding affinities of the THAZ analogues at 5-HT$_{2A}$ and 5-HT$_{2C}$ were determined in [^{3}H]-ketanserin and [^{3}H]mesulergine binding assays to membranes from tsA201 cells transiently expressing the two receptors. The K_D values determined for [^{3}H]ketanserin at 5-HT$_{2A}$ and for [^{3}H]mesulergine at 5-HT$_{2C}$ in saturation binding experiments were in good agreement with previously reported values, as were the K_i values determined for the antagonists mianserin and clozapine (Table 3).[44−46] The K_i values obtained for the reference agonists 5-HT, CP 809101, and MK-212 at the two receptors were considerably higher than their respective EC$_{50}$ values in the Fluo-4/Ca^{2+} and IP-One assays (Tables 1−3). The low binding affinities exhibited by the agonists are likely to arise

dx.doi.org/10.1021/jm301656h | J. Med. Chem. 2013, 56, 1211−1227

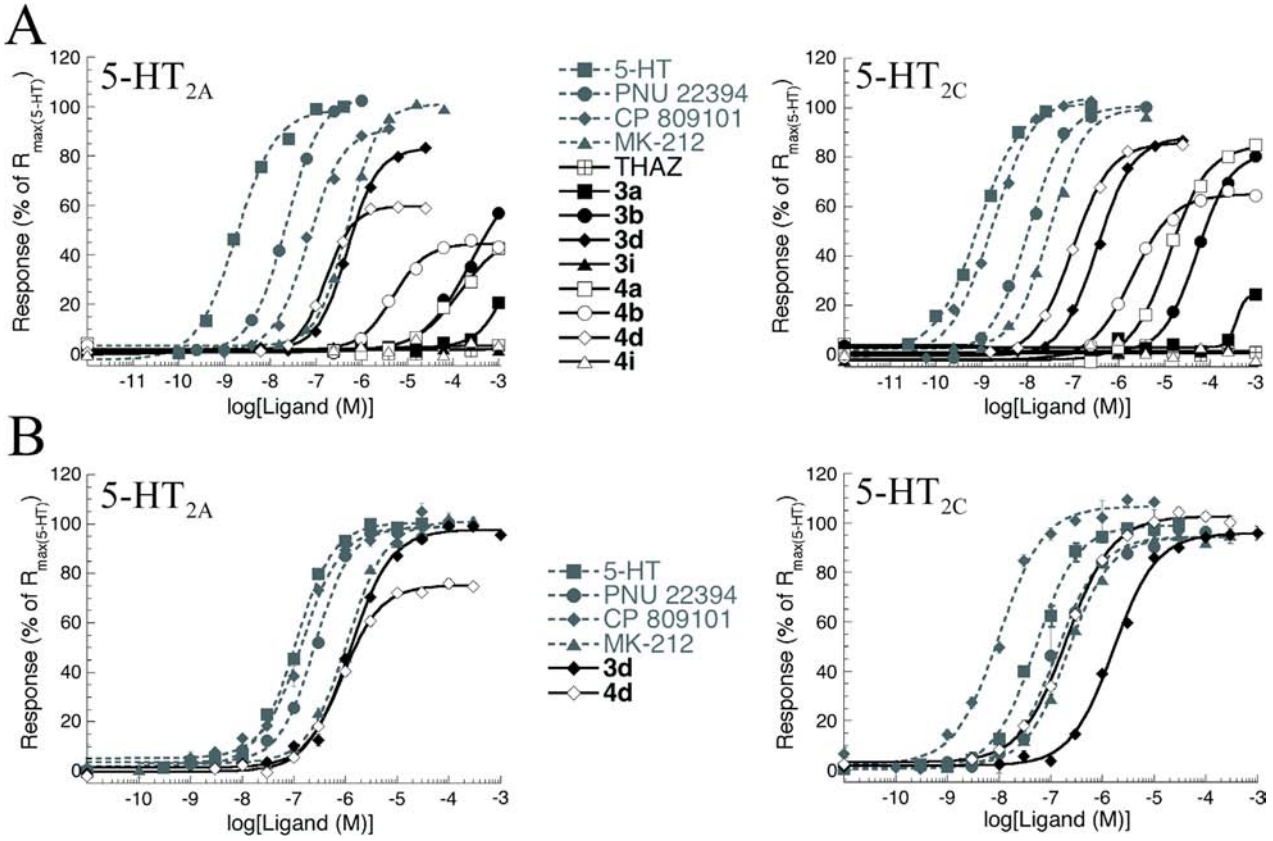

Figure 2. Functional properties of THAZ analogues at human 5-HT$_{2A}$ and 5-HT$_{2C}$ receptors. (A) Concentration−response curves of selected reference ligands and THAZ analogues at the polyclonal 5-HT$_{2A}$- and 5-HT$_{2C}$-HEK293 cell lines in the Fluo-4/Ca^{2+} assay. Error bars are omitted for reasons of clarity (B) Concentration−response curves of 5-HT, PNU-22394, CP 809101, MK-212, and THAZ analogues **3d** and **4d** at the polyclonal 5-HT$_{2A}$- and 5-HT$_{2C}$-HEK293 cell lines in the IP-One assay. Data in B are given as mean ± SEM values. The figures in A and B depict representative experiments performed in duplicate (Fluo-4/Ca^{2+}) or triplicate (IP-One).

Table 2. Functional Properties of Four Reference Agonists and THAZ Analogues 3d and 4d at Polyclonal h5-HT$_{2A}$-HEK293 and h5-HT$_{2C}$-HEK293 Cell Lines in the IP-One Assay[a]

	h5-HT$_{2A}$		h5-HT$_{2C}$	
	EC_{50} [pEC_{50} ± SEM]	R_{max} ± SEM	EC_{50} [pEC_{50} ± SEM]	R_{max} ± SEM
5-HT	0.15 [6.83 ± 0.10]	*100*	0.044 [7.36 ± 0.11]	*100*
PNU 22394	0.21 [6.68 ± 0.08]	98 ± 5	0.12 [6.91 ± 0.06]	97 ± 5
CP 809101	0.14 [6.86 ± 0.06]	90 ± 2	0.0081 [8.09 ± 0.11]	109 ± 7
MK-212	1.2 [5.92 ± 0.09]	101 ± 4	0.16 [6.79 ± 0.10]	93 ± 5
3d	2.4 [5.62 ± 0.09]	95 ± 7	1.7 [5.76 ± 0.08]	92 ± 7
4d	1.3 [5.89 ± 0.06]	77 ± 2	0.23 [6.64 ± 0.05]	105 ± 6

[a]The EC_{50} values are given in μM with pEC_{50} ± SEM values in brackets, and R_{max} ± SEM values are given in % of the R_{max} obtained for 5-HT at the same receptor at the same plate. Data are the means of 4−7 individual experiments performed in triplicate.

from the use of 5-HT$_{2A}$ and 5-HT$_{2C}$ antagonists as radioligands in the assays, since previous studies of 5-HT$_{2A}$[47] and other 7TM receptors[48−51] have found binding affinities of agonists to be highly dependent on the intrinsic activity of the radioligand used.

Analogously to the reference agonists, the K_i values determined for the THAZ analogues at 5-HT$_{2A}$ and 5-HT$_{2C}$ in the [^{3}H]ketanserin and [^{3}H]mesulergine binding assays were markedly higher than their functional EC_{50} values. However, a reasonable correlation existed between the binding affinities determined for the analogues and the agonist potencies displayed by them in the Fluo-4/Ca^{2+} assay (Tables 1 and 3). Whereas **3d** and **4d** displayed low micromolar binding affinities to 5-HT$_{2A}$ and 5-HT$_{2C}$, the other analogues displayed substantially higher K_i values at the receptors (Table 3).

Docking of Selected THAZ Analogues in a Homology Model of the 5-HT$_{2A}$ Receptor. The THAZ analogues **3d**, **4b**, **4d**, and **4i** were docked in our previously published homology model of the 5-HT$_{2A}$ receptor (Figure 3).[52] In the following, residues in the 5-HT$_{2A}$ receptor will be presented with their respective numbers in the amino acid sequence of 5-HT$_{2A}$ as well as with their numbering according to the Ballesteros−Weinstein nomenclature.[53] In the case of both **3d** and **4d**, the charged amino group of the THAZ analogue forms a salt bridge with the D155$^{3.32}$ residue in 5-HT$_{2A}$, the exocyclic oxygen in **3d** and **4d** serves as an acceptor in a hydrogen bond interaction with S239$^{5.43}$, and the *O*- or *N*-benzyl group on the isoxazole ring occupies a hydrophobic region between the transmembrane helices 5 and 6 formed by three aromatic residues (F243$^{5.47}$,

dx.doi.org/10.1021/jm301656h | J. Med. Chem. 2013, 56, 1211−1227

Table 3. Binding Affinities of Reference Ligands and THAZ Analogues in the [^{3}H]Ketanserin and [^{3}H]Mesulergine Competition Binding Assays Using Membranes from tsA201 Cells Transiently Expressing Human 5-HT$_{2A}$ and 5-HT$_{2C}$ Receptors, Respectively[a]

	h5-HT$_{2A}$	h5-HT$_{2C}$
radioligands	K_D ± SEM	K_D ± SEM
[^{3}H]ketanserin	2.9 ± 0.9 nM	nt
[^{3}H]mesulergine	nt	1.4 ± 0.8 nM
	h5-HT$_{2A}$	h5-HT$_{2C}$
reference ligands	K_i [pK_i ± SEM]	K_i [pK_i ± SEM]
5-HT	0.32 [6.49 ± 0.04]	0.079 [7.10 ± 0.04]
CP 809101	0.081 [7.09 ± 0.04]	0.0093 [8.03 ± 0.03]
MK-212	21 [4.68 ± 0.04]	3.4 [5.47 ± 0.08]
mianserin	0.027 [7.57 ± 0.04]	0.0017 [8.76 ± 0.03]
clozapine	0.036 [7.44 ± 0.05]	0.0093 [8.03 ± 0.04]
	h5-HT$_{2A}$	h5-HT$_{2C}$
THAZ analogues	K_i [pK_i ± SEM]	K_i [pK_i ± SEM]
THAZ	>300 [<3.5]	>300 [<3.5]
3a	>300 [<3.5]	>300 [<3.5]
3b	~300 [~3.5]	~300 [~3.5]
3c	~100 [~4.0]	~100 [~4.0]
3d	8.8 [5.06 ± 0.07]	2.3 [5.64 ± 0.06]
3e	nt	7.2 [5.14 ± 0.04]
3f	nt	4.8 [5.32 ± 0.05]
3g	nt	0.31 [6.51 ± 0.04]
3h	>300 [<3.5]	>300 [<3.5]
3i	>300 [<3.5]	>300 [<3.5]
4a	~300 [~3.5]	~300 [~3.5]
4b	~100 [~4.0]	~100 [~4.0]
4d	3.3 [5.48 ± 0.04]	1.2 [5.92 ± 0.05]
4h	>300 [<3.5]	>300 [<3.5]
4i	>300 [<3.5]	>300 [<3.5]

[a]The K_i values are given in μM with pK_i ± SEM values in brackets. Data represents the means of 3−4 individual experiments performed in duplicate. nt, not tested.

W336$^{6.48}$, and F340$^{6.52}$) and three aliphatic residues (V235$^{5.39}$, L236$^{5.40}$,and I344$^{6.56}$) (Figure 3A). The insight into potential reasons for the functional implications arising from methylation of the amino group (Figure 3B) and from different substitutions introduced on the isoxazole ring in the THAZ analogue (Figure 3C) gained from dockings of **4b**, **4i**, and **4d** into the model will be addressed in the Discussion section.

Selectivity Profile of N-Bn-THAZ at Numerous Putative CNS Targets. The selectivity profile of *N*-Bn-THAZ (**3d**) was determined in a broad screening of the ligand at a considerable number of neurotransmitter receptors and transporters as well as at other CNS targets. As can be seen from Supporting Information Table 1, the compound appeared to be quite selective for 5-HT$_{2A}$ and 5-HT$_{2C}$. **3d** was inactive at the third 5-HT$_2$ receptor, 5-HT$_{2B}$, when tested as an agonist, an antagonist, and as a modulator, and displayed no significant binding to and/or functional activity at 5-HT$_{1A}$, 5-HT$_{1B}$, 5-HT$_{1D}$, 5-HT$_3$A, 5-HT$_4$, 5-HT$_6$, or 5-HT$_7$ receptors at concentrations up to 10 μM (Supporting Information Table 1). Furthermore, when tested at a concentrations of 10 μM in binding assays and/or functional assays, **3d** displayed no or negligible activity at a wide range of other 7-TM receptors, including all human dopamine, norepinephrine, histamine, muscarinic, acetylcholine, adenosine, and melatonin receptors or various peptide receptors such as opioid and neurokinin receptors. The compound was also found to be inactive at the monoamine transporters, at miscellaneous ligand-gated and voltage-gated ion channels, and at numerous enzymes including phosphodiesterases and kinases (Supporting Information Table 1).

Development of [^{125}I]-N-(p-I-Bn)-THAZ and Preliminary Characterization of Its Binding to Rat Brain Homogenate and Slices. In an attempt to elucidate the distribution of *N*-Bn-THAZ (**3d**) binding sites in rat CNS and thus enable the identification of other putative targets for the compound, a [^{125}I]-labeled analogue of the compound was developed. The three monoiodinated *N*-Bn-THAZ analogues **3e**, **3f**, and **3g** were synthesized, and their binding affinities to membranes from 5-HT$_{2C}$-expressing tsA201 cells were determined in the [^{3}H]-mesulergine binding assay. Whereas **3e** and **3f** exhibited similar binding affinities to 5-HT$_{2C}$ as **3d**, the *N*-(*p*-I-Bn)-THAZ analogues (**3g**) displayed ~7-fold higher binding affinity, and therefore this analogue was chosen as the candidate for radioligand development (Figure 4A).

Prior to experiments with rat brain tissue or slices, the binding properties of [^{125}I]-*N*-(*p*-I-Bn)-THAZ to membranes from human 5-HT$_{2C}$ receptor-expressing tsA201 cells were investigated (Figure 4B). Because of the low molar concentration of the [^{125}I]-*N*-(*p*-I-Bn)-THAZ stock solution, saturation binding experiments could not be performed. However, when using a concentration of 6 nM [^{125}I]-*N*-(*p*-I-Bn)-THAZ (a ~50-fold lower concentration than the K_i value of **3g** in the [^{3}H]-mesulergine binding assay), the radioligand displayed specific binding to the 5-HT$_{2C}$-expressing tsA201 cell membranes when 100 μM *N*-Bn-THAZ (**3d**) or 10 μM mianserin were used as cold ligands to determine nonspecific binding (Figure 4B).

The ability of [^{125}I]-*N*-(*p*-I-Bn)-THAZ to bind to membranes prepared from four different rat brain regions were investigated. In homogenates of cerebellum, hippocampus, or midbrain, no specific [^{125}I]-*N*-(*p*-I-Bn)-THAZ binding could be determined, neither when using 5-HT, mianserin, and *N*-Bn-THAZ (**3d**) nor *N*-(*p*-I-Bn)-THAZ (**3g**) as cold ligand for the determination of the nonspecific binding (data not shown). In cerebral cortex membranes, total levels of [^{125}I]-*N*-(*p*-I-Bn)-THAZ binding were reduced significantly in a concentration-dependent manner by **3d** and **3g**, displaying pK_i ± SEM values of 6.14 ± 0.06 (n = 3) and 7.99 ± 0.06 (n = 3), respectively (Figure 4C). In contrast, neither 5-HT, mianserin, nor the selective 5-HT$_{2C}$ receptor antagonist SB242084 were able to displace [^{125}I]-*N*-(*p*-I-Bn)-THAZ binding when tested at concentrations up to 50 μM (Figure 4C and data not shown). Furthermore, total levels of [^{125}I]-*N*-(*p*-I-Bn)-THAZ binding to cerebral cortex membranes were found not to be significantly reduced by 300 μM dopamine, 300 μM norepinephrine, 300 μM acetylcholine, 300 μM GABA, 300 μM (*S*)-glutamate, or 1 mM glycine (data not shown).

Autoradiography experiments were performed using 6 nM [^{125}I]-*N*-(*p*-I-Bn)-THAZ binding to frontal levels of cortex and hippocampus/midbrain. Because 5-HT, mianserin, and SB242084 were unable to displace [^{125}I]-*N*-(*p*-I-Bn)-THAZ binding to cerebral cortex membranes to any significant degree (Figure 4C), nonspecific binding was determined in the presence of 100 μM *N*-Bn-THAZ. As shown in Figure 4D, total binding of [^{125}I]-*N*-(*p*-I-Bn)-THAZ could be displaced by excess cold ligand at cortical and midbrain levels indicative of specific binding in these regions, whereas binding was not convincingly reduced at hippocampal levels.

Effects of N-Bn-THAZ in Rodent Assays for Spatial Memory and Psychosis. To examine the effect of *N*-Bn-THAZ (**3d**) on

dx.doi.org/10.1021/jm301656h | J. Med. Chem. 2013, 56, 1211−1227

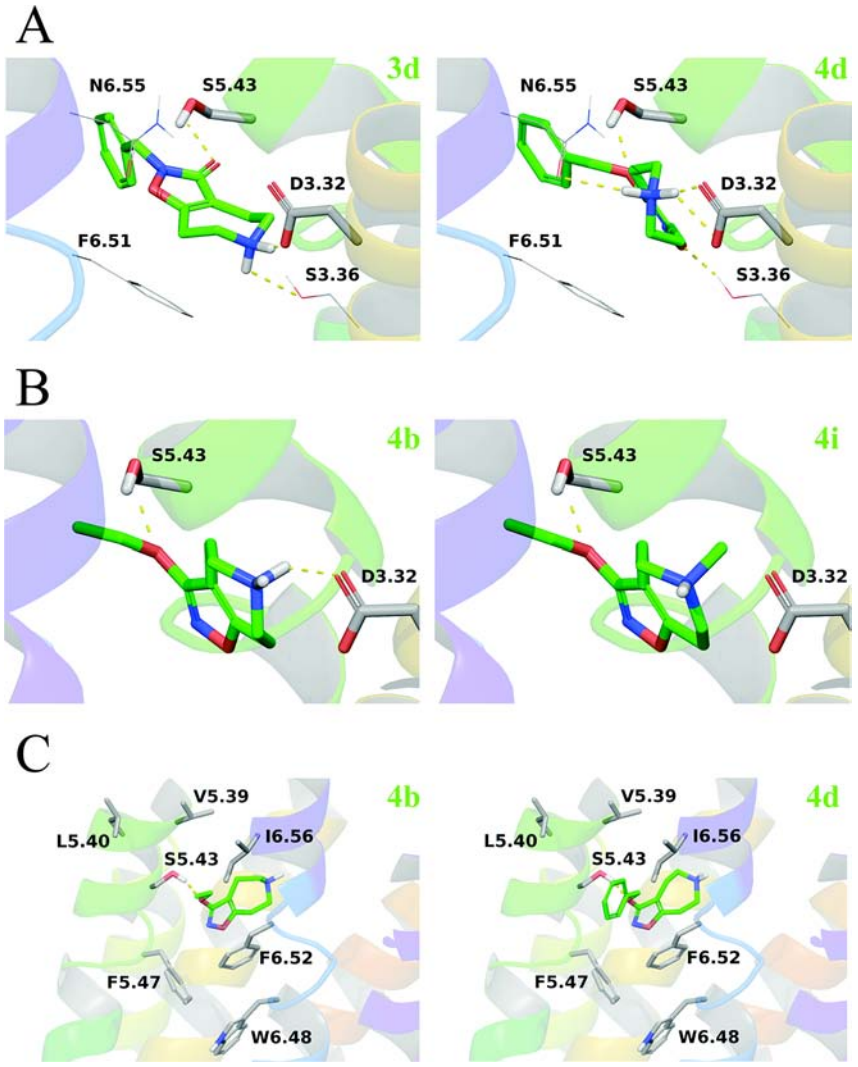

Figure 3. Docking of selected THAZ analogues into a homology model of the 5-HT_{2A} receptor. Receptor residues are given with their numbering according to the Ballesteros–Weinstein nomenclature. (A) Proposed binding modes of **3d** (left) and **4d** (right) in the orthosteric site of 5-HT_{2A}. (B) **4b** (left) and **4i** (right) docked into the orthosteric site of 5-HT_{2A}: Methylation of the amino group in the THAZ analogue is detrimental for its binding to 5-HT_{2A}. (C) **4b** (left) and **4d** (right) docked into the orthosteric site of 5-HT_{2A}: Large hydrophobic substituents on the isoxazole ring of THAZ give rise to higher 5-HT_{2A} affinities by interacting with a hydrophobic region between TM5 and TM6.

learning and memory, we tested the compound in the mouse two-trial place recognition Y-maze, a cognition assay that addresses episodic-like spatial memory formation. In this assay, animals can freely explore two spatially distinct arms of a transparent Y-maze during the acquisition trial and are then exposed, after a flexible inter trial interval (ITI), to the previously explored ("familiar") and one unexplored arm ("novel") for the retrieval trial. The degree to which animals explore the novel over the familiar environment during retrieval is interpreted as an index for the spatial memory formed for the familiar arms.

We first monitored the ability of normal mice to discriminate between novelty and familiarity as a function of increased ITI (10 min, 1 h, 24 h). As shown in Figure 5A, drug naïve mice showed a clear preference for the novel environment 10 min and 1 h after the acquisition, as demonstrated by a significant increase in the distance they traveled in the novel arm during retention (10 min: novel 44.9 ± 11.3%, familiar 25.7 ± 6.5%; $p < 0.05$; *t*-test. 1 h: novel 49.1 ± 9.3%, familiar 26.1 ± 5.1%; $p < 0.05$; *t*-test). This preference was absent 24 h after acquisition (novel 37 ± 5.8%, familiar 31.5 ± 2.9%), indicating that a natural forgetting process had occurred at this time point. Thus, we applied the 24 h ITI to subsequently test the pro-cognitive potential of *N*-Bn-THAZ. Animals treated with 0.43 mg/kg *N*-Bn-THAZ 30 min prior to the acquisition trial showed significantly increased exploration of the novel environment as demonstrated by increased distance traveled (novel 40.4 ± 2.7%, familiar 29.8 ± 1.4%; One-Way ANOVA on ranks: $p < 0.012$), increased number of arm entries (novel 38.5 ± 3%, familiar 30.8 ± 1.5%; $F_{1,16} = 7.513$; $p < 0.05$; NK) and increased time spent (novel 38.8 ± 3.5%, familiar 30.6 ± 1.7%; $F_{1,18} = 5.302$; $p < 0.05$; NK) in the novel arm (Figure 5B–D). To test whether this effect is mediated by the 5-HT_{2C} receptor component of *N*-Bn-THAZ, we treated another group of animals with the selective 5-HT_{2C} receptor antagonist SB242084 (2.1 mg/kg) in addition to 0.43 mg/kg *N*-Bn-THAZ (Figure 5B–D). Co-treatment with SB242084 fully reversed the pro-cognitive effect of *N*-Bn-THAZ with regard to distance traveled (novel 34.7 ± 2.4%, familiar 32.6 ± 1.2%) and number of arm entries (novel 32.8 ± 3.2%, familiar 33.6 ± 1.6%) and also affected the time spent in the novel versus familiar environment (novel 36.6 ± 3.8%, familiar 31.7 ± 1.9%) (Figure

dx.doi.org/10.1021/jm301656h | *J. Med. Chem.* 2013, 56, 1211–1227

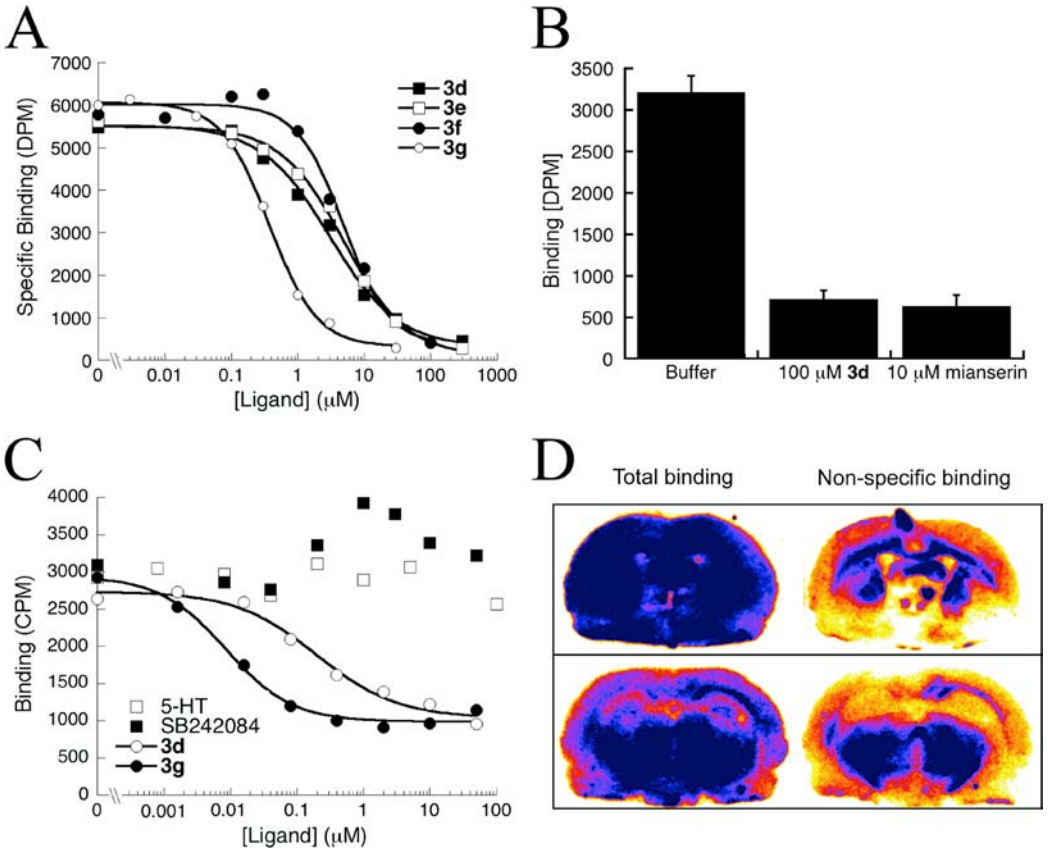

Figure 4. Characterization of the binding properties of [^{125}I]*N*-(*p*-I-Bn)-THAZ. (A) Concentration−inhibition curves for *N*-Bn-THAZ (**3d**) and its iodinated analogues *N*-(*o*-I-Bn)-THAZ (**3e**), *N*-(*m*-I-Bn)-THAZ (**3f**), and *N*-(*p*-I-Bn)-THAZ (**3g**) in the [^{3}H]mesulergine binding assay using membranes from 5-HT$_{2C}$-expressing tsA201 cell membranes. The figure depicts a representative individual experiment (n = 3), and error bars are omitted for clarity. (B) Binding of 6 nM [^{125}I]*N*-(*p*-I-Bn)-THAZ to membranes from 5-HT$_{2C}$-expressing tsA201 cell membranes in the absence (buffer) or presence of 100 μM *N*-Bn-THAZ (**3d**) or 10 μM mianserin. (C) Concentration−inhibition curves for *N*-Bn-THAZ (**3d**) and *N*-(*p*-I-Bn)-THAZ (**3g**) in the [^{125}I]*N*-(*p*-I-Bn)-THAZ binding assay using rat cerebral cortex membranes. 5-HT and SB242084 did not displace [^{125}I]*N*-(*p*-I-Bn)-THAZ (6 nM) binding to the membranes at concentrations up to 50 μM. The figure depicts a representative individual experiment. (D) Autoradiograms showing distribution of [^{125}I]*N*-(*p*-I-Bn)-THAZ binding sites in rat brain. Coronal sections displaying cortical and midbrain regions (top) and cortical and hippocampal regions (bottom) were incubated in the presence of 6 nM [^{125}I]*N*-(*p*-I-Bn)-THAZ for 40 min at room temperature, either in the absence (total binding) or presence of 100 μM *N*-Bn-THAZ (**3d**) (nonspecific binding). The autoradiograms shown are representative slides for two independent experiments performed in triplicate. The sections are represented in a pseudocolor scale that is based on gray scale values. Purple represents the highest levels of binding, while yellow represents the lowest levels. A gray scale image of D is given in Supporting Information Figure 1.

5B−D). These data indicate that *N*-Bn-THAZ bears a pro-cognitive potential on spatial memory formation by strengthening encoding and/or retrieval of spatial information over time.

A few studies have demonstrated efficacy of 5-HT$_{2C}$ receptor agonism in animal models predictive of antipsychotic-like efficacy.[36,54−57] Thus, we tested *N*-Bn-THAZ in the rat conditioned avoidance response (CAR) task. However, we did not observe any effect of the compound in this task at concentrations up to 0.85 mg/kg (data not shown).

DISCUSSION

In the present study, we have applied the structure of the weak glycine and GABA$_A$ receptor antagonist THAZ[28−30] as a scaffold in the development of a novel class of selective and fairly potent 5-HT$_{2A}$/5-HT$_{2C}$ receptor agonists.

Structure−Activity Relationships of the THAZ Analogues at 5-HT$_{2A}$ and 5-HT$_{2C}$ Receptors. The functional properties exhibited by the 12 THAZ analogues at the 5-HT$_{2A}$ and 5-HT$_{2C}$ receptors convey interesting SAR information about this agonist scaffold (Table 1). The complete inactivity of THAZ itself demonstrates that the *O*- or *N*-substituent in the active analogues is a key pharmacophore element for their 5-HT$_{2A}$/5-HT$_{2C}$ activity. Interestingly, direct comparison of the pharmacological properties of the *N*-Me, *N*-Et, and *N*-Bn analogues **3a**, **3b**, and **3d** and those of the corresponding *O*-substituted analogues **4a**, **4b**, and **4d** reveals a shared SAR pattern: both *N*- and *O*-methylation of THAZ induces weak agonistic activity (**3a** and **4a**), which is enhanced further with the introduction of an ethyl group (**3b** and **4b**) and quite dramatically increased in the *N*-Bn and *O*-Bn analogues (**3d** and **4d**). We propose that the massive increases in agonist potencies of **3d** and **4d** (≥30-fold compared to the corresponding *N*-Et and *O*-Et THAZ analogues) are likely to arise from specific interactions of the benzyl ring with the receptor rather than simply introduction of bulk in these positions. The *O*-Bn analogue is a slightly more potent agonist than the *N*-Bn analogue, a trend also observed for the methyl (**3a** and **4a**) and ethyl (**3b** and **4b**) analogues (Table 1). However, the spatial orientations of the phenyl rings of **3d** and **4d** in the orthosteric site could be very similar, with this ring system in the two analogues forming many of the same interactions with the receptor. Thus, the benzyl groups in **3d** and **4d** appears to be of key importance for 5-HT$_{2A}$/5-HT$_{2C}$ activity, and judging from

dx.doi.org/10.1021/jm301656h | J. Med. Chem. 2013, 56, 1211−1227

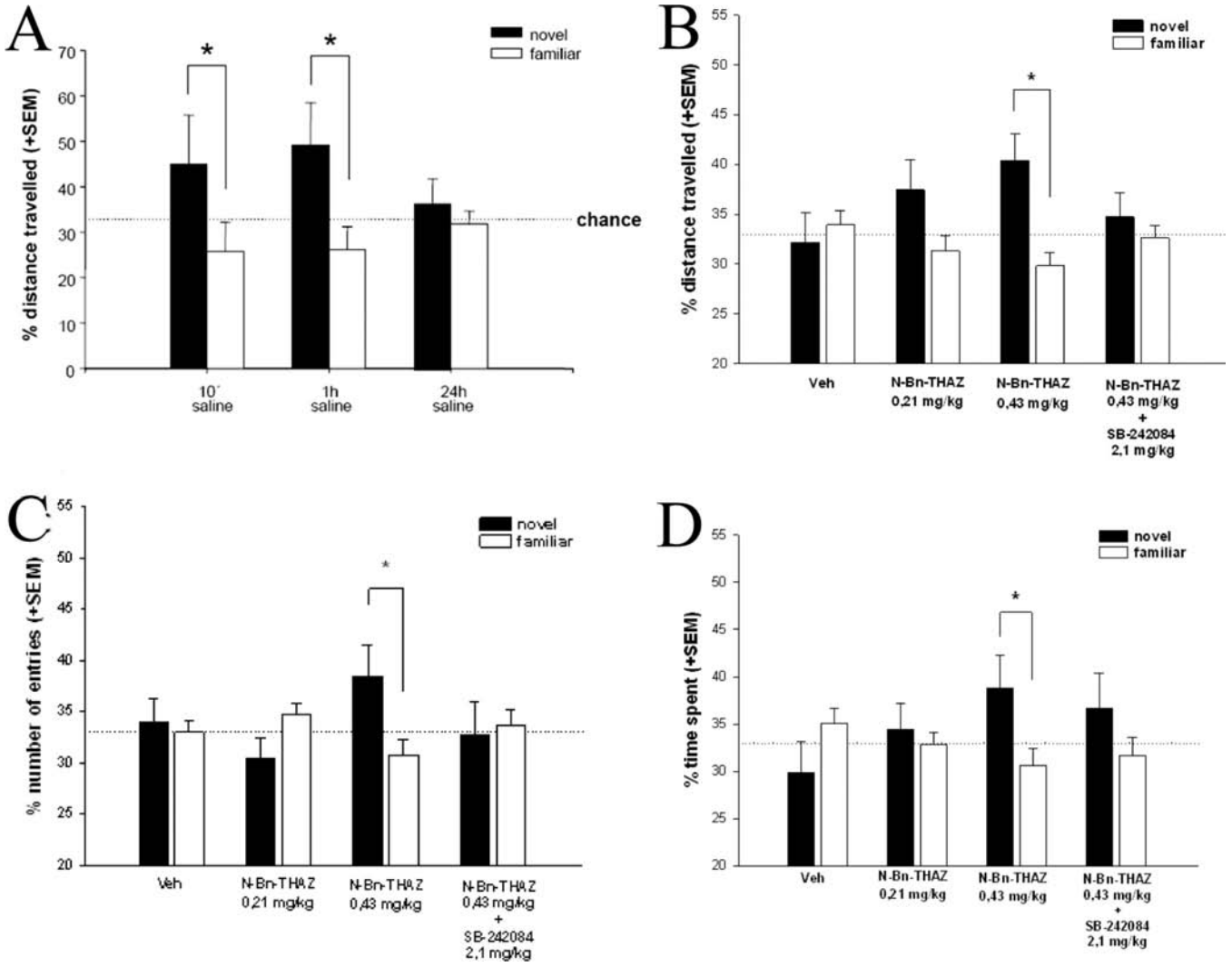

Figure 5. Pro-cognitive effect of *N*-Bn-THAZ (**3d**) on episodic-like spatial memory. (A) Time dependent decay of spatial memory in the 2-trial place recognition Y-maze. Exploration of novel and (pooled) familiar arms measured as distance traveled in the respective areas and shown as mean percentage of total distance traveled. Drug naïve, saline treated animals show significant preference for the novel environment 10 min and 1 h, but not 24 h after acquisition. * $p < 0.05$ versus familiar arm (*t* test ($n = 10$ per group). (B–D) Effect of *N*-Bn-THAZ (**3d**) on spatial discrimination in the 2-trial place recognition Y-maze. Drugs were applied prior to acquisition and memory retention assessed 24 h later. Data are presented as mean percentage of distance traveled (B), number of arms entries (C) and time spent (D) in the novel (white bars) versus familiar (black arms) environment. The effects of *N*-Bn-THAZ (**3d**) for each respective readout were blocked by coadministration of the 5-HT_{2C} selective antagonist SB242084. * $p < 0.05$ versus familiar arms (one-way ANOVA followed by Student–Newman–Keuls (NK) post hoc test) ($n = 10$ per group).

the 7-fold increased 5-HT_{2C} binding affinity of **3g** compared to **3d** in the [^{3}H]mesulergine binding assay (Figure 4A), it may be possible to improve the binding affinity and potency in future THAZ analogues through the introduction of different substituents in the benzyl ring or by substitution of the phenyl ring with other aromatic groups.

The presence of a secondary amino group in the THAZ analogues appears to be another key pharmacophore element for their 5-HT_{2A}/5-HT_{2C} activity. Although tertiary amino group analogues of the more potent THAZ analogues **3d** and **4d** were not included in the series, the detrimental effects of the introduction of a methyl group at the amino function on receptor activity are clear when comparing the functional properties of **3b** and **3i** and those of **4b** and **4i** (Table 1).

The bicyclic isoxazol-3-one tautomeric structure of the THAZ analogue appears to be essential for its 5-HT_{2A}/5-HT_{2C} activity, as none of the *N*- and *O*-substituted THIP, THPO, or THAO analogues exhibit significant activities at the receptors (Table 1).

We propose that analogues with these bicyclic scaffolds are unable to accommodate a low energy conformation in which the 5-HT_{2A}/5-HT_{2C} pharmacophore elements, i.e., the amino group, the exocyclic oxygen, and the isoxazole ring substituent, are positioned as favorable for receptor binding as in the corresponding THAZ analogues. Interestingly, the *N*-substituted THAZ analogue shares some structural similarity with a series of heterocycle-fused azepines recently reported to be potent 5-HT_{2C} receptor agonists.[58] However, in contrast to *N*-Bn-THAZ, most of these analogues, including the 2-benzyl-6,7,8,9-tetrahydro-2*H*-pyridazino[3,4-*d*]azepin-3(5*H*)-one analogue closely related to **3d**, do not exhibit significant selectivity for 5-HT_{2C} over 5-HT_{2B}.[58] This further underlines the subtle structural determinants for these bicyclic compounds in terms of activity and subtype-selectivity profiles at the 5-HT_2 receptors.

Proposed Binding Modes of the THAZ Analogues to the 5-HT_{2A} Receptor. To elucidate the binding modes of the THAZ analogues to the 5-HT_{2A} receptor, **3d**, **4b**, **4d**, and **4i** were

dx.doi.org/10.1021/jm301656h | *J. Med. Chem.* 2013, 56, 1211–1227

docked in our previously published homology model of the 5-HT_{2A} receptor.[52] In view of the lack of selectivity of the THAZ analogues between 5-HT_{2A} and 5-HT_{2C} and the highly conserved orthosteric binding sites of these two receptors, the binding conformations of these analogues in 5-HT_{2C} are likely to be very similar to those in 5-HT_{2A}. Interestingly, the spatial orientations of the two potent agonists from the series in the binding site were found to be somewhat different. Whereas **3d** and **4d** appear to interact with the same receptor residues in their respective binding modes to 5-HT_{2A} and although the orientation of the benzyl groups in the two analogues in the binding site overlap, the orientations of THAZ moieties in the two agonists differ substantially (Figure 3A). The difference in binding mode arises because both analogues span between transmembrane helices 3 and 5, but the alkylbenzyls are located at different positions of the isoxazole rings. The observed detrimental effects of *N*-methylation of the amino group in the THAZ analogue on 5-HT_{2A}/5-HT_{2C} activity seems to be rooted in a disruption of the salt bridge between this group and $D155^{3.32}$ in the receptor (Figure 3B). Thus, we speculate that the spatial orientation of the amino group in the THAZ analogues in the binding site differs from those of the tertiary amino groups in *N*,*N*-diethyl-1-methylpiperidine-4-carboxamide, LSD, and several other 5-HT_2 agonists and perhaps is more similar to the orientations of this group in the binding conformations of other 5-HT_2 agonists with protonated secondary amino groups, including 5-HT.

The projection of the *O*- or *N*-substituents on the isoxazole ring of THAZ into the hydrophobic region formed by residues in transmembrane helices 5 and 6 in the 5-HT_{2A} receptor (Figure 3C) is similar to what has been proposed to contribute to the binding of several other 5-HT_2 ligands. Interactions between hydrophobic ligand substituents and this cavity in the receptor have been associated with agonist activity at 5-HT_{2A},[59] whereas large aromatic ligand substituents projecting into region has been proposed to lead to antagonism of the receptor.[60] From the proposed binding mode of the THAZ analogue to 5-HT_{2A}, it seems feasible that this cavity can accommodate the binding of fairly large, hydrophobic substituents (Figure 3C). Furthermore, introduction of a benzyl group in this region introduces more hydrophobic receptor interactions with the receptor than small aliphatic substituents, which again is in agreement with the dramatically increased 5-HT_{2A}/5-HT_{2C} activity displayed by **3d** and **4d** compared to the Me- and Et-substituted THAZ analogues in the series (Table 1). The key role of the aromatic substituent in **3d** and **4d** for their 5-HT_{2A}/5-HT_{2C} activity will be explored in the design, synthesis, and characterization of future series of THAZ analogues.

***N*-Bn-THAZ Is a Selective 5-HT_{2A} and 5-HT_{2C} Receptor Agonist.** The elaborate in vitro profiling of *N*-Bn-THAZ (**3d**) at numerous putative CNS targets was conducted in part to delineate the selectivity profile of the ligand and in part to search for potential alternative mechanisms underlying its pro-cognitive properties. Interestingly, the compound appears to be quite selective for 5-HT_{2A} and 5-HT_{2C}, exhibiting no significant activity at the other 5-HT receptors tested, at a wide range of other neurotransmitter receptors and transporters or at numerous other CNS targets at a concentration of 10 μM (Supporting Information Table 1). While the 5-HT_{2A}/5-HT_{2C} activity of *N*-Bn-THAZ in itself could give rise to hallucinations and adverse cardiovascular effects,[4,61] the lack of activity of the compound at the 5-HT_{2B} subtype is advantageous from a therapeutic perspective. Interestingly, *N*-Bn-THAZ exhibits weak agonist activity at some muscarinic acetylcholine receptors, including the m_1 subtype, which is closely linked with cognitive functions (Supporting Information Table 1).[62] However, considering that **3d** exhibits ~20-fold higher EC_{50} values at 5-HT_{2A} and 5-HT_{2C} than at m_1 in comparable Ca^{2+} imaging assays and the ability of SB242084 to fully reverse the effect of **3d** in the cognition model strongly suggest that this muscarinic component is unlikely to contribute to the cognition enhancing potential of the compound.

The binding distribution of [^{125}I]-*N*-(*p*-I-Bn)-THAZ in rat brain slices did not shed considerable more light on other putative CNS targets targeted by *N*-Bn-THAZ. On one hand, the preliminary nonquantitative experiments using autoradiography could suggest presence of specific [^{125}I]-*N*-(*p*-I-Bn)-THAZ binding sites for in cortical layers and midbrain regions as the binding here is partly displaceable by *N*-Bn-THAZ (Figure 4D). Such a binding distribution pattern would be in concordance with membrane homogenate binding studies, and the inability of 5-HT to displace [^{125}I]-*N*-(*p*-I-Bn)-THAZ from its native binding sites in homogenate could suggest that the observed binding sites may be distinct from 5-HT_{2A} and 5-HT_{2C} receptors (Figure 4C). On the other hand, the binding distribution could also be ascribed to nonspecific binding of the radioligand, a binding that the closely related *N*-Bn-THAZ is able to reduce, whereas 5-HT and other 5-HT_2 ligands are not. The apparent low 5-HT_{2C} binding affinity of *N*-(*p*-I-Bn)-THAZ (**3g**) (K_i ~ 300 nM in the [^{3}H]mesulergine binding assay) could constitute a problem in terms of obtaining robust [^{125}I]-*N*-(*p*-I-Bn)-THAZ binding intensity as could a potential contamination of cold iodo compound in the radioligand. All in all, this would make the radioligand unsuited for quantitative experiments due to the long exposure times needed (up to four days) and concomitant loss of resolution. In conclusion, [^{125}I]-*N*-(*p*-I-Bn)-THAZ appears not to be a suitable tool radioligand for mapping native 5-HT_{2A}/5-HT_{2C} binding sites. In view of these difficulties in interpreting the data and because the pro-cognitive effects of *N*-Bn-THAZ appear to be convincingly explained by an involvement of 5-HT_{2C} receptors (see below), we will refrain from speculations about putative additional targets for the ligand.

***N*-Bn-THAZ Is an Efficient Bioavailable Cognitive Enhancer.** The impact of 5-HT_{2C} receptor modulation on cognition remains a matter of debate, with recent studies providing rather conflicting evidence on the beneficial effect of either agonism or antagonism.[22] In the present study, we investigated the effect of *N*-Bn-THAZ (**3d**) on spatial recognition memory in mice in the two-trial place recognition Y-maze (Figure 5). In contrast to other classical tests of spatial learning and memory, such as the Morris water maze, this learning task avoids the use of appetitive or aversive reinforcers that may trigger nonspecific effects. Moreover, it does not require extensive training procedures before addressing mnemonic processes. Administering the compound to mice prior to the encoding phase restored delay-induced spatial memory impairment during the retrieval phase. This effect was fully reversed by coadministration of a selective 5-HT_{2C} antagonist, indicating that *N*-Bn-THAZ mediates its effects via 5-HT_{2C} receptor agonism and suggesting a central role for 5-HT_{2C} receptors in spatial learning. As the compounds were dosed prior to the acquisition trial, the pro-cognitive effect observed during retrieval is due to a potentiation of either the encoding phase, the consolidation phase, or both. Three different parameters were examined as measures for the exploration of novelty versus familiarity, namely "distance travelled", "time spent", and "number of arm entries". The factors time spent and distance traveled reflect "inspective"

exploration, whereas the number of arm entries (encounter with novelty) corresponds more to "inquisitive" exploration.[63] While it has been suggested that drugs can affect these parameters in opposite ways,[63] *N*-Bn-THAZ exhibited beneficial effects on both parameters. One disadvantage of measuring the time spent in a given arm of the Y-maze is that it does not distinguish between active exploration and nonrelated behavior (e.g., grooming, freezing). Thus, analyzing distance traveled is a more accurate readout of inspective behavior.

A cognition enhancing potential of 5-HT_{2C} agonists has been addressed recently utilizing different compounds in rodents with CP 809101 improving object recognition memory[36] and Ro 60-0175 enhancing attention.[64] The present study is thus in line with the recent literature but is, to our knowledge, the first report of a beneficial effect of a 5-HT_{2C} agonist on spatial learning. In general, increased levels of acetylcholine and dopamine elicited by 5-HT_{2C} agonism have been ascribed to such cognition promoting efficacy,[65] but it should be noted that 5-HT_{2C} antagonists have been reported to bear pro-cognitive potential as well.[66] Thus, the efficacy and underlying mechanisms might depend on the brain regions involved in the task and the chosen animal model of cognitive impairment. In any case, the effect described here underlines the mnemonic potential of *N*-Bn-THAZ on hippocampus-dependent spatial memory, and it will be of interest to address other cognitive domains as well as the potential to *N*-Bn-THAZ and other THAZ analogues to reverse cognitive deficits in animal disease models of cognitive impairment and dementia in future studies.

CONCLUSION

In summary, the *N*- and *O*-benzyl-substituted THAZ analogues constitute a novel class of bioavailable and CNS accessible 5-HT_{2A}/5-HT_{2C} receptor agonists characterized by pronounced selectivity for these receptors over a plethora of other targets. This adds yet another interesting chapter to the story of the medicinal chemistry versatility of the bicyclic 3-isoxazole, which also constitutes the scaffold of several interesting pharmacological tool compounds targeting ionotropic glutamate receptors, $GABA_A$ receptors, and GABA transporters.[27,67,68] While more potent and equally selective agonists for 5-HT_{2A} and 5-HT_{2C} receptors certainly exist, it may very well be possible to increase the agonist potencies of *N*-Bn-THAZ (**3d**) and *O*-Bn-THAZ (**4d**) by future development, whereas it remains to be seen if the 5-HT_{2A} and 5-HT_{2C} activity in the THAZ analogue can be effectively separated. The cognition enhancement displayed by **3d** in the spatial memory assay is highly interesting, and the apparent key role of 5-HT_{2C} for this pro-cognitive potential in the compound supports the notion of this receptor being involved in processes underlying learning and memory proposed in previous studies. Besides the obvious therapeutic potential in this cognitive enhancement, it could be interesting to apply **3d**, **4d** or analogues of these as pharmacological tools in future studies aimed at unraveling the physiological roles and therapeutic prospects in 5-HT_{2A} and 5-HT_{2C} receptors.

EXPERIMENTAL SECTION

Chemistry. *General Procedures.* All reagents and solvents were purchased from Aldrich and used without further purification. All air- and moisture-sensitive reactions were performed under a nitrogen atmosphere using syringe-septum cap techniques and flame-dried glassware. Thin layer chromatography was carried out on Merck silica gel 60 F_{254} plates, and detection took place using UV (254 and 366 nm) or $KMnO_4$ spray reagent. Flash column chromatography (FC) was performed on Merck silica gel (0.040−0.063 mm), and for dry column vacuum chromatography (DCVC)[32] Merck silica gel (0.015−0.040 mm) was applied. Unless otherwise stated, DCVC was performed using the solvents EtOAC and heptane with concentrations of EtOAc varying from 0−100% with 5% increments. Melting points were recorded on a Büchner instrument or on a SRS optimelt apparatus and were uncorrected. ^1H and ^{13}C NMR was recorded on a 300 MHz Varian Mercury 300BB equipped with a 5 mm 1H{BB} probe, a 300 Varian Gemini 2000BB spectrometer equipped with a 5 mm ^{31}P, $^{13}C\{^1H, ^{19}F\}$ probe or a Bruker Avance 400 MHz spectrometer equipped with a 5 mm PABBO BB$\{^1H, ^{19}F\}$ Z-GRD probe, at 300 K. Data are tabulated in the following order: chemical shift (δ) [multiplicity (b, broad; s, singlet; d, doublet; t, triplet; q, quartet; sept, septet; m, multiplet), coupling constant(s) *J* (Hz), number of protons]. The solvent residual peak was used as internal reference.[69] Elemental analyses were performed at Analytical Research Department, H. Lundbeck A/S Denmark, or by J. Theiner, Department of Physical Chemistry, University of Vienna, Austria. Preparative and analytical reverse phase HPLC of the radioligand were performed on a Waters Breeze HPLC system equipped with a binary pump system, dual wavelength detector, and a Carroll Ramsey S105 in-line radiodetector based on a silicon diode. Separation was achieved using a Phenomenex Luna (2) C-18 (250 mm × 4.6 mm) column and a standard binary buffer system with a flow of 1 mL/min: buffer A (4.9% acetonitrile, 95% water, 0.1% trifluoroacetic acid), buffer B (99.9% acetonitrile, 0.1% trifuoroacetic acid). Preparative separation was achieved using the following gradient: 0−3 min (0% B); 3−35 min (gradient to 60% B); 35−37 min (gradient to 100% B); 37−40 min (100% B); 40−41 min (gradient to 0% B); 41−45 min (0% B). Analytical separation and analysis was performed using the gradient: 0−15 min (gradient from 0% to 100% B); 15−20 min (100% B); 20−21 min (gradient to 0% B); 21−25 min (0% B). The purity of all tested compounds was established using combustion analysis or analytical HPLC. The elemental analysis calculated values are within 0.4% of the found values, and the HPLC purity is ≥95% unless otherwise stated.

General Procedure for O- and N-Alkylation. To a solution of **8**[32] (for **10b**, **11b**), **9**[28] (for **12a−g**, **13a−g**), **14**,[28] (for **16a−c**, **17a−c**), or **15**[32] (for **18c**) (1 equiv) in acetone (14 mL/g) was added potassium carbonate (2.5 equiv), and the mixture was refluxed for 30 min. To this mixture was added the appropriate alkyl or phenylalkyl halide (1.1 equiv). The reaction mixture was refluxed for 24 h, filtered, and evaporated. The resulting residue was subjected to FC or DCVC.

*2-Ethyl-3-oxo-2,3,4,5,6,7-hexahydroisoxazolo[5,4-c]pyridin-6-ium Fumarate (**1b**).* Using the general procedure for alkylation of **8** and ethyl bromide as the alkyl halide, the two isomeric products: Methyl 2-ethyl-3-oxo-2,3,4,5-tetrahydroisoxazolo[5,4-*c*]pyridine-6(7*H*)-carboxylate (**10b**) (0.45 g, 21%) and methyl 3-ethoxy-4,5-dihydroisoxazolo[5,4-*c*]pyridine-6(7*H*)-carboxylate (**11b**) (0.29 g, 14%) were obtained. A solution of **10b** (0.84 g, 3.1 mmol) in HCl in AcOEt (2.8N, 4 mL) was left at room temperature until a clear solution appeared and then evaporated. The residue was added aqueous KOH (2N, 3 mL) and water (10 mL). The mixture was extracted with CH_2Cl_2 (3 × 15 mL). The combined organic phases were dried ($MgSO_4$), filtered, and evaporated. This residue was dissolved in Et_2O (10 mL), and a solution of fumaric acid (0.22 g, 1.9 mmol) in 2-propanol (4 mL) was added to give the product as colorless crystals (0.41 g, 55%): mp 136−137 °C. ^1H NMR (400 MHz, MeOD-d_4): δ 6.69 (s, 1H), 3.98−3.92 (m, 4H), 3.16 (t, *J* = 5.8 Hz, 2H), 2.45 (tt, *J* = 5.8, 1.7 Hz, 2H), 1.29 (t, *J* = 7.1 Hz, 3H). ^{13}C NMR (101 MHz, MeOD-d_4): δ 170.7, 167.7, 166.0, 136.0, 107.2, 42.77, 42.64, 41.6, 19.1, 12.9. Anal. ($C_8H_{12}N_2O_2 \cdot 0.5C_4H_4O_4 \cdot 0.33H_2O$) C, H, N.

*3-Ethoxy-4,5,6,7-tetrahydroisoxazolo[5,4-c]pyridin-6-ium Fumarate (**2b**).* A solution of **11b** (0.6 g, 2.2 mmol) in HCl in EtOH (4N, 11 mL) was left at room temperature until a clear solution appeared and then evaporated. To the residue was added aqueous sodium carbonate (2N, 15 mL), and the mixture was extracted with CH_2Cl_2 (3 × 25 mL). The combined organic phases were dried ($MgSO_4$), filtered, and evaporated. This residue was dissolved in Et_2O (10 mL), and a solution of fumaric acid (0.23 g, 2.0 mmol) in 2-propanol (5 mL) was added. The precipitated crude of the product was recrystallized (MeCN−EtOH) to give the product (0.37 g, 72%): mp 137−141 °C. ^1H NMR (400 MHz,

dx.doi.org/10.1021/jm301656h | J. Med. Chem. 2013, 56, 1211−1227

MeOD-d_4): δ 4.36 (t, J = 1.6 Hz, 2H), 4.32 (q, J = 7.1 Hz, 2H), 3.49 (t, J = 6.1 Hz, 2H), 2.72 (tt, J = 6.1, 1.6 Hz, 2H), 1.42 (t, J = 7.1 Hz, 3H). ^{13}C NMR (101 MHz, MeOD-d_4): δ 170.5, 161.6, 102.9, 67.4, 42.7, 41.6, 16.9, 14.8. Anal. ($C_8H_{12}N_2O_2 \cdot 0.5C_4H_4O_4 \cdot 0.5H_2O$) C, H, N.

*2-Methyl-3-oxo-3,4,5,6,7,8-hexahydro-2H-isoxazolo[4,5-d]-azepin-6-ium Bromide (**3a**).* Using the general procedure for alkylation of **9** and methyl iodide as the alkyl halide, the two isomeric products:, methyl 2-methyl-3-oxo-4,5,7,8-tetrahydro-2*H*-isoxazolo[4,5-*d*]azepine-6(3*H*)-carboxylate (**12a**) (5.30 g, 41%) and methyl 3-methoxy-7,8-dihydro-4*H*-isoxazolo[4,5-*d*]azepine-6(5*H*)-carboxylate (**13a**) (5.35 g, 42%), were obtained. A solution of **12a** (3.50 g, 1.6 mmol) in a solution of HBr in AcOH (33%, 35 mL) was left at room temperature for 48 h and then evaporated. The residue was recrystallized (MeOH−Et_2O) to give 3.19 g (83%) of the desired product: mp 171.0−173.0 °C. ^{1}H NMR (300 MHz, $CDCl_3$/MeOD-d_4): δ 3.85 (b s, 2H), 3.43 (t, J = 6.6 Hz, 2H), 3.17 (t, J = 5.7 Hz, 2H), 2.81 (t, J = 5.7 Hz, 2H). Anal. ($C_8H_{12}N_2O_2 \cdot$HBr) C, H, N.

*3-Methoxy-7,8-dihydro-4H-isoxazolo[4,5-d]azepine-6-ium Chloride (**4a**).* A solution of **13a** (0.68 g, 3.0 mmol) in a solution of KOH in MeOH (4N, 6 mL) was left at room temperature for 8 h and evaporated. To the residue was added water (10 mL) and extracted with $CHCl_3$ (5 × 30 mL). The combined organic phases were dried ($MgSO_4$), filtered, and evaporated. The residue was dissolved in a solution of HCl in AcOEt (2.8N, 15 mL) and stirred at room temperature. The product was isolated as crystals (297 mg, 44%): mp 201−202 °C. ^{1}H NMR (400 MHz, MeOD-d_4): δ 3.96 (s, 3H), 3.47−3.44 (m, 2H), 3.43−3.40 (m, 2H), 3.21−3.17 (m, 2H), 2.77−2.73 (m, 2H). ^{13}C NMR (101 MHz, MeOD-d_4): δ 171.7, 169.2, 105.6, 57.7, 48.6, 45.8, 25.8, 18.8. Anal. ($C_8H_{12}N_2O_2 \cdot$HCl) C, H, N.

*2-Ethyl-3-oxo-3,4,5,6,7,8-hexahydro-2H-isoxazolo[4,5-d]azepin-6-ium Fumarate (**3b**).* Using the general procedure for alkylation of **9** and ethyl iodide as the alkyl halide, the two isomeric products, methyl 2-ethyl-3-oxo-4,5,7,8-tetrahydro-2*H*-isoxazolo[4,5-*d*]azepine-6(3*H*)-carboxylate (**12b**) (0.94 g, 49%) and methyl 3-ethoxy-7,8-dihydro-4*H*-isoxazolo[4,5-*d*]azepine-6(5*H*)-carboxylate (**13b**) (0.58 g, 30%), were obtained. A solution of **12b** (5.15 g, 24 mmol) in a solution of HBr in AcOH (33%, 30 mL) was left at room temperature for 72 h and then evaporated. The residue was dissolved in water (30 mL), and upon addition of sodium carbonate (6 g) the mixture was extracted with $CHCl_3$ (3 × 50 mL). The combined organic phases were dried ($MgSO_4$), filtered, and evaporated. This residue was dissolved in a mixture of EtOH (2 mL) and Et_2O (20 mL), and a solution of fumaric acid (1.86 g, 16.0 mmol) in 2-propanol (25 mL) was added. The precipitated crude of the product was recrystallized (MeOH−Et_2O) to give the product (4.12 g, 65%): mp 174−176 °C. ^{1}H NMR (300 MHz, $CDCl_3$): δ 6.73 (s, 2H), 3.92 (q, J = 7.1 Hz, 2H), 3.24 (t, J = 5.1 Hz, 2H), 3.18 (t, J = 5.7 Hz, 2H), 2.96 (t, J = 6.3 Hz, 2H), 2.64 (t, J = 5.7 Hz, 2H). Anal. ($C_9H_{14}N_2O_2 \cdot C_4H_4O_4$) C, H, N.

*3-Ethoxy-7,8-dihydro-4H-isoxazolo[4,5-d]azepine-6-ium Chloride (**4b**).* Prepared as described for **4a** from **13b**. The product was isolated as crystals (0.60 g, 66%): mp 202−203 °C. ^{1}H NMR (400 MHz, MeOD-d_4): δ 4.27 (q, J = 7.1 Hz, 2H), 3.47−3.41 (m, 4H), 3.21−3.17 (m, 2H), 2.77−2.73 (m, 2H), 1.40 (t, J = 7.1 Hz, 3H). ^{13}C NMR (101 MHz, MeOD-d_4): δ 171.0, 168.9, 105.7, 67.1, 48.6, 45.8, 25.8, 18.8, 14.8. Anal. ($C_9H_{14}N_2O_2 \cdot$HCl) C, H, N.

*2-Propyl-3-oxo-3,4,5,6,7,8-hexahydro-2H-isoxazolo[4,5-d]-azepin-6-ium Fumarate (**3c**).* Using the general procedure for alkylation of **9** and propyl bromide as the alkyl halide, the two isomeric products, methyl 2-propyl-3-oxo-4,5,7,8-tetrahydro-2*H*-isoxazolo[4,5-*d*]azepine-6(3*H*)-carboxylate (**12c**) (0.49 g, 64%) and methyl 3-propoxy-7,8-dihydro-4*H*-isoxazolo[4,5-*d*]azepine-6(5*H*)-carboxylate (**13c**) (0.21 g, 28%), were obtained. A solution of **12c** (1.01 g, 4.0 mmol) in HBr in AcOH (33%, 8 mL) was left at room temperature for 72 h and then evaporated. The residue was suspended in aqueous NaOH (1N, 20 mL), and the mixture was extracted with CH_2Cl_2 (3 × 25 mL). The combined organic phases were washed with a saturated aqueous solution of $NaHCO_3$ (25 mL), dried ($MgSO_4$), filtered, and evaporated. This residue was dissolved in 2-propanol (4 mL), and a solution of fumaric acid (0.46 g, 3.9 mmol) in 2-propanol (4 mL) was added. The precipitate of the crude product was recrystallized (MeOH−Et_2O) to give the product (0.87 g, 70%): mp 189 °C (decomp). ^{1}H NMR (D_2O): δ 6.61 (s, 2H), 3.87 (t, J = 6 Hz, 2H), 3.3−3.5 (m, 4H), 3.07 (t, J = 5 Hz, 2H), 2.65 (t, J = 5 Hz, 2H), 1.5−1.8 (m, 2H), 0.80 (t, J = 5 Hz, 2H). Anal. ($C_{10}H_{16}N_2O_2 \cdot C_4H_4O_4$) C, H, N.

*2-Benzyl-3-oxo-3,4,5,6,7,8-hexahydro-2H-isoxazolo[4,5-d]-azepin-6-ium Fumarate (**3d**).* Using the general procedure for alkylation of **9** and benzyl iodide as the alkyl halide, the two isomeric products, methyl 2-benzyl-3-oxo-4,5,7,8-tetrahydro-2*H*-isoxazolo[4,5-*d*]azepine-6(3*H*)-carboxylate (**12d**) (0.94 g, 49%) and methyl 3-benzyloxy-7,8-dihydro-4*H*-isoxazolo[4,5-*d*]azepine-6(5*H*)-carboxylate (**13d**) (0.58 g, 30%) were obtained. A solution of **12d** (3.75g, 12 mmol) in HBr in AcOH (33%, 8 mL) was left at room temperature for 72 h, evaporated, and worked up as described for **3c**. To a solution of crude amine (2.39 g, 10 mmol) in 2-propanol (5 mL) was added a solution of fumaric acid (1.16 g, 10 mmol) in 2-propanol (10 mL). The precipitate was recrystallized (MeOH−Et_2O) to give the title compound as crystals (3.14 g, 70%): mp 152 °C (decomp). ^{1}H NMR (300 MHz, MeOD-d_4): δ 7.29−7.33 (m, 5H), 6.66 (s, 2H), 5.06, (s, 2H), 3.31−3.39 (m, 4H), 3.00 (t, J = 5.7 Hz, 2H), 2.69 (t, J = 5.7 Hz, 2H). Anal. ($C_{14}H_{16}N_2O_2 \cdot C_4H_4O_4$) C, H, N.

*3-Benzyloxy-7,8-dihydro-4H-isoxazolo[4,5-d]azepine-6-ium Chloride (**4d**).* Prepared as described for **4a** from **13d**. The product was isolated and recrystallized (EtOH−AcOEt) (0.6 g, 53%): mp 139−140 °C. ^{1}H NMR (400 MHz, MeOD-d_4): δ 7.47−7.42 (m, 2H), 7.41−7.34 (m, 3H), 5.26−5.24 (s, 2H), 3.42−3.34 (m, 4H), 3.16−3.12 (m, 2H), 2.73−2.69 (m, 2H). Anal. ($C_{14}H_{16}N_2O_2 \cdot$HCl$\cdot 0.5H_2O$) C, H, N.

*2-(2-Iodobenzyl)-3-oxo-3,4,5,6,7,8-hexahydro-2H-isoxazolo[4,5-d]azepin-6-ium Bromide (**3e**).* Using the general procedure for alkylation of **9** and 2-iodobenzyl bromide as the alkyl halide, the two isomeric products, methyl 2-(2-iodobenzyl)-3-oxo-4,5,7,8-tetrahydro-2*H*-isoxazolo[4,5-*d*]azepine-6(3*H*)-carboxylate (**12e**) (0.26 g, 42%) and methyl 3-(2-iodobenzyloxy)-7,8-dihydro-4*H*-isoxazolo[4,5-*d*]-azepine-6(5*H*)-carboxylate (**13e**) (0.33 g, 54%), were obtained. A mixture of **12e** (0.33 g, 0.78 mmol) in HBr in AcOH (33%, 5 mL) was refluxed for 20 h at 110 °C. The reaction mixture was evaporated and recrystallized (MeOH−ether) to give (0.33, 79%). ^{1}H NMR (300 MHz, $CDCl_3$): δ 7.89 (d, J = 7.8 Hz, 1H), 7.37 (t, J = 7.5 Hz, 1H), 7.22 (dd, J = 1.5, 7.8 Hz, 1H), 7.06 (dt, J = 1.5, 7.5 Hz, 1H), 5.08 (s, 2H), 3.38−3.44 (m, 4H), 3.01 (t, J = 5.7 Hz, 2H), 2.71 (t, J = 6.0 Hz, 2H). ^{13}C NMR (75 MHz, $CDCl_3$): δ 167.4, 166.5, 140.4, 136.2, 130.9, 130.3, 129.4, 109.3, 97.9, 67.1, 54.9, 47.3, 44.3, 25.0, 18.4 ppm. Anal. ($C_{14}H_{15}N_2O_2I \cdot$HBr$\cdot 0.5H_2O$) C, H, N.

*2-(3-Iodobenzyl)-3-oxo-3,4,5,6,7,8-hexahydro-2H-isoxazolo[4,5-d]azepin-6-ium Bromide (**3f**).* Using the general procedure for alkylation of **9** and 3-iodobenzyl bromide as the alkyl halide, the two isomeric products, methyl 2-(3-iodobenzyl)-3-oxo-4,5,7,8-tetrahydro-2*H*-isoxazolo[4,5-*d*]azepine-6(3*H*)-carboxylate (**12f**) (0.20 g, 33%) and methyl 3-(3-iodobenzyloxy)-7,8-dihydro-4*H*-isoxazolo[4,5-*d*]azepine-6(5*H*)-carboxylate (**13f**) (0.40 g, 66%), were obtained. A mixture of **12f** (0.40 g, 0.93 mmol) in HBr in AcOH (33%, 5 mL) was refluxed for 20 h at 110 °C. Recrystallization (MeOH−Et_2O) gave **3f** as colorless crystals (0.43 g, 74%). ^{1}H NMR (300 MHz, D_2O): δ 6.56 (b s, 1H,), 6.50 (b d, J = 7.8 Hz, 1H), 6.21 (b d, J = 8.1 Hz, 1H), 6.02 (t, J = 7.8 Hz, 1H), 3.81 (s, 2H), 2.30−2.42 (m, 4H), 1.95 (b t, J = 5.4 Hz, 2H), 1.68 (b t, J = 5.7 Hz, 2H). ^{13}C NMR (75 MHz, $CDCl_3$): δ 167.6, 166.9, 137.9, 137.1, 137.0, 131.5, 127.9, 109.3, 95.5, 67.2, 49.5, 47.3, 44.3, 25.2, 18.5 ppm. Anal. ($C_{14}H_{15}N_2O_2I \cdot$HBr$\cdot 0.5H_2O$) C, H, N.

*2-(4-Iodobenzyl)-3-oxo-3,4,5,6,7,8-hexahydro-2H-isoxazolo[4,5-d]azepin-6-ium Bromide (**3g**).* Using the general procedure for alkylation of **9** and 4-iodobenzyl bromide as the alkyl halide, the two isomeric products, methyl 2-(4-iodobenzyl)-3-oxo-4,5,7,8-tetrahydro-2*H*-isoxazolo[4,5-*d*]azepine-6(3*H*)-carboxylate (**12g**) (0.32 g, 53%) and methyl 3-(4-iodobenzyloxy)-7,8-dihydro-4*H*-isoxazolo[4,5-*d*]-azepine-6(5*H*)-carboxylate (**13g**) (0.40 g, 33%), were obtained. A mixture of **12g** (0.40 g, 0.93 mmol) in HBr in AcOH (33%, 5 mL) was refluxed for 20 h at 110 °C. Recrystallization (MeOH−Et_2O) gave **3g** as colorless crystals (0.26 g, 59%). ^{1}H NMR (300 MHz, D_2O): δ 7.72 (b d, J = 8.1 Hz, 2H), 7.06 (b d, J = 8.1 Hz, 2H), 5.03 (s, 2H), 3.38−3.50 (m, 4H), 3.06 (b t, J = 6.0 Hz, 2H), 2.71 (b t, J = 5.7 Hz, 2H). ^{13}C NMR (75

MHz, $CDCl_3$): δ 167.5, 166.7, 138.4, 134.3, 130.4, 109.3, 94.3, 44.4, 25.1, 18.5 ppm. Anal. ($C_{14}H_{15}N_2O_2I$·HBr·1.5H_2O) C, H, N.

*2,6-Dimethyl-3-oxo-3,4,5,6,7,8-hexahydro-2H-isoxazolo[4,5-d]-azepin-6-ium Chloride (**3h**).* A solution of **3a** (2.50 g, 10 mmol) in water (30 mL), adjusted to pH ca. 12 by addition of K_2CO_3, was extracted with CH_2Cl_2 (3 × 50 mL). The combined organic phases were evaporated and the residue dissolved in a mixture of aqueous solutions of formic acid (98%, 25 mL) and formaldehyde (40%, 25 mL). This solution was refluxed for 4 h and then evaporated. A mixture of the residue and water (8 mL) adjusted to pH 12 by addition of K_2CO_3, was extracted with $CHCl_3$ (3 × 100 mL). The combined organic phases were dried ($MgSO_4$), filtered, and evaporated. This residue was dissolved in EtOAc (5 mL), and upon addition of a solution of HCl in EtOAc (1N, 10 mL), crude product precipitated. Recrystallization (EtOH−Et_2O) afforded 1.45 g (66%) of the title compound: mp 215 °C (decomp). ^{1}H NMR (300 MHz, MeOD-d_4): δ 6.71 (s, 2H), 3.61 (b t, *J* = 1.5 Hz, 2H), 3.50 (s, 3H), 2.88 (t, *J* = 5.7 Hz, 2H), 2.59 (s, 3H), 2.45 (dt, *J* = 1.5, 5.7 Hz, 2H). Anal. ($C_9H_{14}N_2O_2$·HCl) C, H, N.

*6-Methyl-3-methoxy-7,8-dihydro-4H-isoxazolo[4,5-d]azepine-6-ium Chloride (**4h**).* Prepared as described for **3h**. The product was isolated and recrystallized (MeOH−AcOEt) (0.24 g, 62%): mp 179 °C (decomp). ^{1}H NMR (400 MHz, MeOD-d_4): δ 3.96 (s, 3H), 3.54 (b s, 4H), 3.22 (t, *J* = 5.8 Hz, 2H), 3.03 (s, 3H), 2.78 (t, *J* = 5.7 Hz, 2H). ^{13}C NMR (101 MHz, MeOD-d_4): δ 171.5, 168.7, 105.3, 57.83, 57.73, 54.9, 44.1, 24.4, 17.6.Anal. ($C_9H_{14}N_2O_2$·HCl) C, H, N.

*2-Ethyl-6-methyl-3-oxo-3,4,5,6,7,8-hexahydro-2H-isoxazolo[4,5-d]azepin-6-ium Fumarate (**3i**).* The *N*-methylation of **3b** (0.89 g, 3.0 mmol) was accomplished following a procedure analogous with that described for **3h**. To a solution of the crude free amine of **3i** (0.54 g, 2.8 mmol) in 2-propanol (2 mL) was added a solution of fumaric acid (0.32 g, 2.8 mmol) in 2-propanol (5 mL). Upon addition of Et_2O (5 mL), crude fumaric salt slowly precipitated. Recrystallization (MeOH−Et_2O) afforded **3i** as crystals (0.99 g, 66%): mp 126.0−128.0 °C. ^{1}H NMR (300 MHz, MeOD-d_4): δ 6.68 (s, 2H), 3.92, (q, *J* = 7.2 Hz, 2H), 3.28 (b t, *J* = 6.3 Hz, 2H), 3.21 (b t, *J* = 5.7 Hz, 2H), 3.01 (t, *J* = 5.7 Hz, 2H), 2.79 (s, 3H), 2.61 (t, *J* = 5.7 Hz, 2H). Anal. ($C_{10}H_{16}N_2O_2$·$C_4H_4O_4$) C, H, N.

*6-Methyl-3-ethoxy-7,8-dihydro-4H-isoxazolo[4,5-d]azepine-6-ium Fumarate (**4i**).* Prepared as described for **3i**. The product was isolated and recrystallized (MeOH−Et_2O) (0.52 g, 61%): mp 129−130 °C. ^{1}H NMR (400 MHz, MeOD-d_4): δ 6.70 (s, 2H), 4.26 (q, *J* = 7.1 Hz, 2H), 3.40−3.32 (m, *J* = 5.0 Hz, 4H), 3.17−3.12 (m, 2H), 2.88 (s, 3H), 2.72−2.68 (m, 2H), 1.40 (t, *J* = 7.1 Hz, 3H). ^{13}C NMR (101 MHz, MeOD-d_4): δ 170.9, 170.6, 169.3, 135.9, 105.8, 67.0, 57.7, 54.9, 44.1, 25.1, 18.2, 14.9. Anal. ($C_{10}H_{16}N_2O_2$·$C_4H_4O_4$) C, H, N.

*2-Methyl-3-oxo-2,3,4,5,6,7-hexahydroisoxazolo[4,5-c]pyridin-5-ium Chloride (**5a**).* To a solution of **14** (0.96 g, 4 mmol) in Et_2O (20 mL) was added CH_2N_2 (1.65 mmol). The reaction mixture was stirred overnight at room temperature added AcOH (2 mL) and evaporated. FC gave the two isomers: methyl 2-methyl-3-oxo-2,3,6,7-tetrahydroisoxazolo[4,5-*c*]pyridine-5(4*H*)-carboxylate (**16a**) (0.33 g, 32%) and methyl 3-methoxy-6,7-dihydroisoxazolo[4,5-*c*]pyridine-5(4*H*)-carboxylate (**17a**) (0.39 g, 38%). **5a** was prepared from **16a** using the method described for **3h**. The product was isolated and recrystallized (MeOH−AcOEt) (0.14 g, 86%): 152.1−153.2. ^{1}H NMR (400 MHz, MeOD-d_4): δ 4.01 (t, *J* = 1.7 Hz, 2H), 3.60 (t, *J* = 6.2 Hz, 2H), 3.55 (s, 3H), 2.98 (tt, *J* = 6.2, 1.6 Hz, 2H). ^{13}C NMR (101 MHz, MeOD-d_4): δ 165.84, 165.80, 103.0, 41.8, 39.0, 33.2, 21.2. Anal. ($C_7H_{12}N_2O_2$·HCl) C, H, N.

*3-Methoxy-4,5,6,7-tetrahydroisoxazolo[4,5-c]pyridin-5-ium Fumarate (**6a**).* Prepared from **17a** using the method described for **1b**. The product was isolated and recrystallized (MeOH−EtO_2) (0.127 g, 62%): 192−195 (decomp). ^{1}H NMR (400 MHz, MeOD-d_4): δ 4.09 (t, *J* = 1.5 Hz, 2H), 3.99 (s, 3H), 3.58 (t, *J* = 6.2 Hz, 2H), 3.06 (tt, *J* = 6.2, 1.5 Hz, 2H). ^{13}C NMR (101 MHz, MeOD-d_4): δ 170.2, 166.7, 99.1, 57.9, 42.1, 39.2, 21.6. Anal. ($C_7H_{12}N_2O_2$·$C_4H_4O_4$) C, H, N.

*2-Ethyl-3-oxo-2,3,4,5,6,7-hexahydroisoxazolo[4,5-c]pyridin-5-ium Fumarate (**5b**).* Using the general procedure for alkylation of **14** and ethyl bromide as the alkyl halide, the two isomeric products, methyl 2-ethyl-3-oxo-2,3,6,7-tetrahydroisoxazolo[4,5-*c*]pyridine-5(4*H*)-carboxylate (**16b**) (2.8 g, 41%) and methyl 3-ethoxy-6,7-dihydroisoxazolo-[4,5-*c*]pyridine-5(4*H*)-carboxylate (**17b**) (3.37 g, 50%), were obtained. **5b** was prepared from **16b** as described for **3d**. The product was isolated and recrystallized (MeOH−EtO_2) (1.9 g, 48%): 161.4−163.1. ^{1}H NMR (400 MHz, MeOD-d_4): δ 6.70 (s, 3H), 4.01−3.96 (m, 4H), 3.56 (t, *J* = 6.2 Hz, 2H), 2.97 (tt, *J* = 6.2, 1.6 Hz, 2H), 1.31 (t, *J* = 7.1 Hz, 3H). ^{13}C NMR (101 MHz, MeOD-d_4): δ 170.4, 166.2, 165.5, 135.8, 103.5, 42.7, 41.7, 38.9, 21.4, 13.0. Anal. ($C_8H_{12}N_2O_2$·1.5$C_4H_4O_4$) C, H, N.

*2-Benzyl-3-oxo-2,3,4,5,6,7-hexahydroisoxazolo[4,5-c]pyridin-5-ium Fumarate (**5c**).* Using the general procedure for alkylation of **14** and benzyl bromide as the alkyl halide, the two isomeric products, methyl 2-benzyl-3-oxo-2,3,6,7-tetrahydroisoxazolo[4,5-*c*]pyridine-5(4*H*)-carboxylate (**16c**) (10.0 g, 69%) and methyl 3-benzyloxy-6,7-dihydroisoxazolo[4,5-*c*]pyridine-5(4*H*)-carboxylate (**17c**) (2.3 g, 16%), were obtained. **5c** was prepared from **16c** as describe for **1b**. The product was isolated and recrystallized (MeOH−EtO_2) (0.82 g, 45%): mp 166−168 °C. ^{1}H NMR (400 MHz, MeOD-d_4): δ 7.36−7.31 (m, 5H), 6.69 (s, 2H), 5.09 (s, 2H), 3.91 (t, *J* = 1.7 Hz, 2H), 3.44 (t, *J* = 6.1 Hz, 2H), 2.83 (tt, *J* = 6.1, 1.7 Hz, 2H). ^{13}C NMR (101 MHz, MeOD-d_4): δ 170.7, 167.2, 166.0, 136.00, 135.94, 129.8, 129.40, 129.23, 104.4, 50.9, 41.8, 39.0, 21.9.Anal. ($C_{13}H_{14}N_2O_2$·$C_4H_4O_4$) C, H, N.

*3-Benzyloxyoxy-4,5,6,7-tetrahydroisoxazolo[4,5-c]pyridin-5-ium Chloride (**6c**).* Prepared from **17c** as describe for **4a**. The product was isolated and recrystallized (MeCN−EtO_2) (1.4 g, 34%): mp 196−197 °C. ^{1}H NMR (400 MHz, MeOD-d_4): δ 7.47−7.44 (m, 2H), 7.41−7.35 (m, 3H), 5.29 (s, 2H), 4.10 (t, *J* = 1.5 Hz, 2H), 3.58 (t, *J* = 6.2 Hz, 2H), 3.05 (tt, *J* = 6.2, 1.5 Hz, 2H). ^{13}C NMR (101 MHz, MeOD-d_4): δ 169.5, 166.7, 136.9, 129.73, 129.60, 129.58, 99.3, 73.1, 42.2, 39.3, 21.7.Anal. ($C_{13}H_{14}N_2O_2$·HCl) C, H, N.

*2-Benzyl-3-oxo-3,4,5,6,7,8-hexahydro-2H-isoxazolo[4,5-c]azepin-5-ium Fumarate (**7c**).* Using the general procedure for alkylation of **15** and benzyl bromide as the alkyl halide, the two isomeric products, methyl 2-benzyl-3-oxo-4,6,7,8-tetrahydro-2*H*-isoxazolo[4,5-*c*]azepine-5(3*H*)-carboxylate (**18c**) (0.4 g, 47%) and the *O*-benzyl isomer methyl 3-(benzyloxy)-7,8-dihydro-4*H*-isoxazolo[4,5-*c*]azepine-5(6*H*)-carboxylate (0.21 g, 28%), were obtained. **7c** was prepared from **18c** using the method describe for **1b**. The product was isolated and recrystallized (MeOH−Et_2O) (0.28 g, 51%): mp 139−142 °C. ^{1}H NMR (400 MHz, MeOD-d_4): δ 7.38−7.30 (m, 5H), 6.69 (s, 2H), 5.08 (s, 2H), 4.00 (s, 2H), 3.50−3.47 (m, 2H), 2.90−2.86 (m, 2H), 2.10−2.04 (m, 2H). ^{13}C NMR (101 MHz, MeOD-d_4): δ 173.1, 170.9, 166.9, 136.04, 135.88, 129.9, 129.4, 129.2, 105.4, 50.9, 50.2, 40.2, 27.4, 23.4. Anal. ($C_{14}H_{16}N_2O_2$·$C_4H_4O_4$) C, H, N.

*Methyl 2-(Tributylstannylbenzyl)-3-oxo-4,5,7,8-tetrahydro-2H-isoxazolo[4,5-d]azepine-6(3H)-carboxylate (**19**).* **12g** (0.28 g, 0.7 mmol) and tetrakis(triphenylphosphine)palladium(0) (0.084 mg, 0.06 mmol) was dissolved in dry toluene (40 mL) and bis(tributyltin) (0.66 mL, 1.3 mmol) was added under a N_2 atmosphere. The reaction mixture was refluxed for 22 h followed by evaporation and DCVC, which gave the title compound as a colorless oil (157 mg, 41%). ^{1}H NMR (300 MHz, $CDCl_3$): δ 7.42 (b. d, *J* = 7.8 Hz, 2H), 7.24 (b d, *J* = 8.1 Hz, 2H), 4.95 (s, 2H), 3.72 (s, 3H), 3.52−3.66 (m, 4H), 2.68−2.80 (m, 2H), 2.51−2.62 (m, 2H). ^{13}C NMR (75 MHz, $CDCl_3$): δ 167.4, 167.2, 155.9, 142.0, 136.8, 134.3, 127.5, 109.8, 109.4, 52.9, 49.8, 48.4, 45.6, 29.2, 28.7, 27.5, 22.4, 13.9, 10.2. Anal. HPLC purity ≥99%.

*Methyl 2-(4-Iodobenzyl)-3-oxo-4,5,7,8-tetrahydro-2H-isoxazolo-[4,5-d]azepine-6(3H)-carboxylate (**12g** from **19**).* Chloramine-T trihydrate (0.36 g, 1.3 mmol) was suspended in a solution of EtOAc−DMF−AcOH (50 mL, 94:5:1) and water (0.4 mL). The solution was added to **19** (27 mg, 0.045 mmol), followed by a solution of NaI (7 mg, 0.047 mmol) in phosphate buffered saline (2 mL). The reaction mixture was stirred at room temperature for 25 min and quenched by adding $Na_2S_2O_3$ (0.25 g, 1.3 mmol). The reaction mixture was washed with water (6 × 10 mL), dried ($MgSO_4$), filtered, and evaporated. DCVC gave **12g** (13.5 mg, 71%). ^{1}H NMR as described for **12g** from **9**.

*[^{125}I]2-(4-Iodobenzyl)-3-oxo-3,4,5,6,7,8-hexahydro-2H-isoxazolo-[4,5-d]azepin-6-ium Bromide (**21**).* Chloramine-T trihydrate (41 mg) was suspended in a mixture of EtOAc (4.75 mL), DMF (0.25 mL), acetic acid (50 μL), and water (50 μL). Of this solution, 1 mL was added to the precursor **19** (2.1 mg) in a 2 mL HPLC vial, and shortly after carrier-free [^{125}I] NaI (20 μL, 44.0 MBq) was added. When the reaction was

dx.doi.org/10.1021/jm301656h | J. Med. Chem. 2013, 56, 1211−1227

finished, NaS_2O_3 (9.4 mg in 300 μL water) was added to quench excess of chloramine-T and the reaction mixture was washed with water (3 × 300 μL). The organic layer was evaporated to dryness under a gentle helium flow to give **20**. Subsequently, a solution of HBr in acetic acid (33%, 500 μL) was added to the vial, and the reaction was left for 5 h. The reaction mixture was cooled on ice and slowly neutralized with a solution of aqueous NaOH (4N, 500 μL), and the pH was adjusted to approximately 7. This mixture was subjected to reverse phase HPLC for purification. The desired product was collected in the interval 22.0−22.3 min. The product, **21**, was measured to an activity of 40.3 MBq (RCY: 91%) and analyzed to have a radiochemical purity of 100% and a specific activity of 94 Ci/mmol. The moderate specific activity was due to traces of cold iodide compound used in the preparation of the stannyl precursor. The HPLC fraction was diluted with 5× ultrapurified water then applied onto a preactivated C-18 Sep-PAK (160 mg). It was then washed with ultra purified water (5 mL), eluted with 1% AcOH in EtOH (5 mL), and subsequently diluted to a concentration of approximately 5 MBq/ml with water.

Pharmacology. Materials. Culture media, serum, antibiotics and buffers for cell culture were obtained from Invitrogen (Paisley, UK). The Fluo−4/AM dye was obtained from Molecular Probes (Eugene, OR), and the IP-One assay kit was purchased from Cisbio (Bagnols, France). [^{3}H]Mesulergine ([N^6-methyl-^{3}H]mesulergine) and [^{3}H]ketanserine were purchased from GE Healthcare (Buckinghamshire, UK). 5-HT and probenecid were purchased from Sigma-Aldrich (St. Louis, MO), asenapine was purchased from Ascent Scientific (Bristol, UK), and PNU-22394, Ro 60-0175, CP 809101, MK-212, WAY 161503, clozapine, mianserin, and MDL 11,939 were purchased from Tocris Cookson (Bristol, UK). SB242084 were synthesized in-house at H. Lundbeck A/S. The cDNAs encoding for the human 5-HT_{2A} (variant 1) and human 5-HT_{2C} (isoform INI) were generous gifts from Dr. Hans Bräuner-Osborne.

Construction of Stable Cell Lines and General Cell Culture. Polyclonal h5-HT_{2A}- and h5-HT_{2C}-HEK293 cell lines were generated essentially as previously described.[70] Cells were transfected with pCDNA3.1-h5-HT_{2A} or pCDNA3.1-h5-HT_{2C} plasmids using PolyFect (Qiagen, West Sussex, UK) as a DNA carrier and cultured in culture medium [Dulbecco's Modified Eagle Medium supplemented with penicillin (100 U/mL), streptomycin (100 μg/mL), and 5% dialyzed fetal bovine serum] supplemented with 2 mg/mL G418 for four weeks before use. The tsA201 cells and the stable h5-HT_{2A}- and h5-HT_{2C}-HEK293 cell lines were maintained at 37 °C in a humidified 5% CO_2 incubator in culture medium (for the stable cell lines the medium was supplemented with 1 mg/mL G-418).

Fluo-4/Ca^{2+} Assay. The functional characterization of 10 reference ligands and the THAZ analogues at the h5-HT_{2A}- and h5-HT_{2C}-HEK293 cell lines in the Fluo-4/Ca^{2+} assay was performed essentially as previously described.[71] The cells were split into poly-D-lysine-coated black 96-well plates with clear bottom (6×10^4 cells/well). The following day, the culture medium was aspirated and the cells were incubated in 50 μL of assay buffer [Hank's Buffered Saline Solution (HBSS) containing 20 mM HEPES, 1 mM $CaCl_2$, 1 mM $MgCl_2$, and 2.5 mM probenecid, pH 7.4] supplemented with 6 mM Fluo−4/AM at 37 °C for 1 h. Then the buffer was aspirated, the cells were washed once with 100 μL of assay buffer, and then 100 μL of assay buffer was added to the cells (in the antagonist experiments the antagonist was added at this point). The 96-well plate was assayed in a FLEXStation^3 (Molecular Devices, Crawley, UK) measuring emission [in fluorescence units (FU)] at 525 nm caused by excitation at 485 nm before and up to 90 s after addition of 33.3 μL of agonist solution in assay buffer. The compounds were characterized in duplicate at least three times at each cell line. The antagonist experiments were performed using an EC_{75}−EC_{85} concentrations of 5-HT as agonist.

IP-One Assay. The functional charaterization of ligands at the h5-HT_{2A}- and h5-HT_{2C}-HEK293 cell lines in the IP-One assay was performed essentially as described previously.[43] On the day of the experiment, subconfluent h5-HT_{2A}- and h5-HT_{2C}-HEK293 cells were washed one time with phosphate-buffered saline and detached from the cell culture plate using dissociation buffer (Sigma-Aldrich). Cells were centrifuged and resuspended in assay buffer (HBSS supplemented with 20 mM HEPES, 1 mM $CaCl_2$, and 1 mM $MgCl_2$, pH 7.4) at a concentration of 1×10^7 cells/mL. Ligand solutions were prepared in HBSS supplemented with 1 mM $CaCl_2$, 1 mM $MgCl_2$, and 40 mM LiCl. Then 5 μL of ligand solution was mixed with 5 μL of cell suspension in a white 384-well OptiPlate (PerkinElmer, Waltham, MA, USA). The plate was sealed and incubated at 37 °C for 1 h, followed by 15 min incubation at room temperature. Next, 10 μL of detection reagents (lysis buffer containing 2.5% Eu^{3+}-anti-IP_1 antibody and 2.5% IP_1-d2) was added and the plate was incubated for 1 h at room temperature. The plate was read on an Envision (PerkinElmer, Waltham, MA) exciting the cells with light at 340 nm and measuring emitted light at 615 and 665 nm. In this assay, the time-resolved-fluorescence resonance energy transfer 665 nm/615 nm ratio is inversely proportional to the IP_1 accumulation in the cells upon 5-HT_{2A} or 5-HT_{2C} receptor activation. The compounds were characterized in triplicate at least four times at each cell line.

[^{3}H]Ketanserin, [^{3}H]Mesulergine, and [^{125}I]-*N*-(*p*-I-Bn)-THAZ Binding Assays. Competition binding to membranes from tsA201 cells transiently expressing human 5-HT_{2A} and 5-HT_{2C} receptors using [^{3}H]ketanserin and [^{3}H]mesulergine as radioligands, respectively, was performed essentially as previously described.[44,72] The cells were transfected with pCDNA3.1-h5-HT_{2A} or pCDNA3.1-h5-HT_{2C} using PolyFect as a DNA carrier 36−48 h prior to the experiments. On the day of the assay, the cells were harvested and scraped into assay buffer [50 mM Tris-HCl supplemented with 5 mM $CaCl_2$ (pH 7.4) for 5-HT_{2A} and 50 mM Tris-HCl (pH 7.4) for 5-HT_{2C}], homogenized using an Ultra-Turrax for 10 s, and centrifuged for 20 min at 50000*g*. The resulting pellets were resuspended in fresh assay buffer, homogenized, and centrifuged at 50000*g* for another 20 min, after which the pellet was resuspended in assay buffer and used for the binding experiments.

In the saturation binding experiments, the cell membranes were incubated with various [^{3}H]ketanserin or [^{3}H]mesulergine concentrations in the absence (total binding) or in the presence of 10 μM mianserin (nonspecific binding). In the competition binding experiments, cell membranes were incubated with a fixed radioligand concentration (2 nM [^{3}H]ketanserin or 0.5 nM [^{3}H]mesulergine) and various concentrations of the test compounds. A total binding assay volume of 1000 μL was used, and nonspecific binding was determined in reactions with 10 μM mianserin. The binding reactions were incubated for 1 h at 37 °C. Whatman GF/C filters were presoaked for 1 h in a 0.2% polyethyleneimine solution, and binding was terminated by filtration through these filters using a 48-well cell harvester and washing with 3 × 4 mL ice-cold isotonic NaCl solution. Following this, the filters were dried, 3 mL of Opti-Fluor (Packard) was added, and the amount of bound radioactivity was determined in a scintillation counter. The fraction of specifically bound radioligand was always <5% of the total amount of radioligand. The binding experiments were performed in duplicate at least three times for each compound at each receptor.

Competition binding studies with [^{125}I]-*N*-(*p*-I-Bn)-THAZ (specific activity 94 Ci/mmol) was performed to membranes from tsA201 cells transiently expressing human 5-HT_{2C} or to rat brain membranes prepared from cortex, cerebellum, hippocampus, and midbrain dissections and prepared using standard procedures.[73] The binding assay was performed exactly as the [^{3}H]ketanserin and [^{3}H]mesulergine binding assays, except for the use of a different assay buffer [50 mM Tris-HCl, 10 mM $MgSO_4$, 0.5 mM EDTA, 0.1% ascorbic acid, 0.1% BSA (pH 7.4)] and an assay concentration of 6 nM [^{125}I]-*N*-(*p*-I-Bn)-THAZ as radioligand. Nonspecific binding was determined with 10 μM mianserin in the experiments with the tsA201 cell membranes, whereas 10 μM mianserin or 1 mM *N*-Bn-THAZ were used to determine nonspecific binding in the experiments with the rat brain membranes.

Cryostat Sectioning and [^{125}I]-*N*-(*p*-I-Bn)-THAZ Autoradiography. Brains from male Sprague−Dawley rats (250−300 g; Charles River, Germany) were sectioned on a cryostat in 20 μm coronal sections at −25 °C (corresponding to bregma 4.5−4.8 mm),[74] thaw-mounted onto gelatinized glass slides, allowed to dry, and stored at −80 °C until analyzed. Autoradiography was carried out using a protocol highly similar to previously described using the same buffer as described for homogenate binding studies.[75] Frozen tissue sections were warmed to room temperature, then preincubated for 30 min at room temperature in buffer under constant gentle shaking. For determination of total binding,

sections were incubated in buffer containing 6 nM [^{125}I]-*N*-(*p*-I-Bn)-THAZ for 40 min at room temperature under constant gentle shaking. Sections used for nonspecific binding included 100 μM 2-Bn-THAZ. Sections were washed for 2 × 20 s in ice-cold buffer followed by 20 s in ice-cold double-distilled H_2O. Slides were dried at room temperature in a gentle air stream for 1 h. They were then fixed in paraformaldehyde vapor overnight at 4 °C. The sections were dried for 3 h in a desiccator at room temperature, followed by exposure to a ^{125}I-sensitive BAS-2040 phosphor imaging plate (Science Imaging Scandinavia AB, Nacka, Sweden) for 4 days at 4 °C. The imaging plate was scanned on a BAS-2500 bioimaging analyzer (Fujifilm Europe GmbH, Düsseldorf, Germany). The autoradiograms were analyzed with ImageJ V.1.38j (http://rsbweb.nih.gov/ij/).

Two-Trial Place Recognition Y-Maze. Eight weeks old, male C57Bl/6J mice (Charles River, Germany) were used in the place recognition Y-maze task. Animals were housed in pairs in a temperature and humidity controlled environment on a 12 h (6:00−18:00 h) light cycle with free access to water and food. The task has been adapted from earlier reports with slight adaptations described in the following.[76,77] The maze consisted of transparent plastic shaped to a Y with each arm arranged in a 120° angle to each other and measuring 32 cm × 14 cm × 8 cm ($L \times H \times W$). The maze was placed on an airflow table. Guillotine doors were mounted at the center of the maze to allow blockade of each arm independently. Moreover, fixed and nontransparent walls were mounted on the outside of the maze in between each two arms to block free view from one arm into the other. Different visual cues were mounted outside of the arms, thus out of reach for the animals, making each arm's visual environment distinct from the others. During the acquisition trial, subjects were placed in the middle of the maze with all three doors closed and subsequently allowed to freely explore two arms ("familiar") for 3 min. Animals were then removed manually and returned to their home cage for the duration of the intertrial interval (ITI). Following the ITI, subjects were placed back into the center of the maze (with all three doors initially closed) for the retention trial and then allowed to freely explore all three arms for 3 min. The arm previously closed during acquisition was designated as "novel" during retention. All movement was videotracked by a ceiling-mounted CCD camera and data transferred to a tracking software EthoVision3.0 (Noldus, Netherlands) for trace analysis. *N*-Bn-THAZ (dissolved in 0.9% NaCl) was applied orally (po) and SB242084 (dissolved in 10% HP-betaCD) subcutaneously (sc), both 30 min prior to the acquisition trial. The vehicle group was dosed with 10% HP-betaCD, po, 30 min before acquisition. All doses stated in the results part refer to free base. Data are expressed as the mean value ± SEM, and a one-way ANOVA was applied to test for statistical differences between exploration of familiar and novel arms (SigmaStat 3.0, Aspire Software, USA). Data from the two familiar arms were not significantly different from each other and pooled. All in vivo experiments were performed in accordance with the Danish legislation, and animals were treated with adherence to the guidelines for the care of experimental animals.

Docking of Ligands into a 5-HT$_{2A}$ Receptor Homology Model. The THAZ analogues **3d**, **4b**, **4d**, and **4i** were docked in our 5-HT$_{2A}$ receptor homology model.[52] A docking grid was generated using Glide 5.8.[78] An enclosed box of default size was defined around the Asp^{155} (D155$^{3.32}$) residue in the receptor. Docking was carried out using Glide 5.8,[78] with XP precision. Ten poses per ligand were kept. For each ligand, the highest ranked pose where interactions with transmembrane helices 3 and 5 were observed was selected for each compound.

■ ASSOCIATED CONTENT

Ⓢ Supporting Information

Supporting Information Table 1: Data from the screening of *N*-Bn-THAZ (**3d**) at numerous putative targets. Supporting Information Figure 1: A grey scale version of Figure 4D. This material is available free of charge via the Internet at http://pubs.acs.org.

■ AUTHOR INFORMATION

Corresponding Author

*Phone: +45 39179650. Fax: +45 35336041. E-mail: aaj@sund.ku.dk.

Notes

The authors declare no competing financial interest.

■ ACKNOWLEDGMENTS

This study was supported by the Aase and Ejner Danielsen Foundation, the Direktør Ib Henriksen Foundation, the Lundbeck Foundation, the Carlsberg Foundation, the Danish Medical Research Council, and the Novo Nordisk Foundation. Dr. Hans Bräuner-Osborne is thanked for providing us with the pCDNA3.1-h5-HT$_{2A}$ and pCDNA3.1-h5-HT$_{2C}$ plasmids, and Dr. Gitte Moos Knudsen is thanked for providing access to autoradiography equipment. Ulla Geneser is thanked for technical assistance with the synthetic work, and M.Sc. Lenea Nørskov-Lauritsen and M.Sc. Stine Engesgaard Jacobsen are thanked for their kind guidance in connection with the performance of the IP-One assay.

■ ABBREVIATIONS USED

5-HT, 5-hydroxytryptamine (serotonin); 7-TM, 7-transmembrane; CAR, conditioned avoidance response; GABA$_A$, γ-aminobutyric acid type A; CNS, central nervous system; IP$_1$, inositol monophosphate; ITI, inter trial interval; LSD, lysergic acid diethylamide; NK, Newman−Keuls; THAO, 5,6,7,8-tetrahydro-4*H*-isoxazolo[4,5-*c*]azepin-3-ol; THAZ, 5,6,7,8-tetrahydro-4*H*-isoxazolo[4,5-*d*]azepin-3-ol; THIP, 4,5,6,7-tetrahydroisoxazolo[5,4-*c*]pyridin-3-ol; THPO, 4,5,6,7-tetrahydroisoxazolo[4,5-*c*]pyridin-3-ol

■ REFERENCES

(1) Berger, M.; Gray, J. A.; Roth, B. L. The expanded biology of serotonin. *Annu. Rev. Med.* **2009**, *60*, 355−366.

(2) Monti, J. M.; Jantos, H. The roles of dopamine and serotonin, and of their receptors, in regulating sleep and waking. *Prog. Brain Res.* **2008**, *172*, 625−646.

(3) Gershon, M. D.; Tack, J. The serotonin signaling system: from basic understanding to drug development for functional GI disorders. *Gastroenterology* **2007**, *132*, 397−414.

(4) Ramage, A. G.; Villalon, C. M. 5-Hydroxytryptamine and cardiovascular regulation. *Trends Pharmacol. Sci.* **2008**, *29*, 472−481.

(5) Moltzen, E. K.; Bang-Andersen, B. Serotonin reuptake inhibitors: the corner stone in treatment of depression for half a century—a medicinal chemistry survey. *Curr. Top. Med. Chem.* **2006**, *6*, 1801−1823.

(6) Gray, J. A.; Roth, B. L. The pipeline and future of drug development in schizophrenia. *Mol. Psychiatry* **2007**, *12*, 904−922.

(7) Katzman, M. A. Current considerations in the treatment of generalized anxiety disorder. *CNS Drugs* **2009**, *23*, 103−120.

(8) Goadsby, P. J. Serotonin receptor ligands: treatments of acute migraine and cluster headache. *Handb. Exp. Pharmacol.* **2007**, 129−143.

(9) Halford, J. C.; Harrold, J. A.; Boyland, E. J.; Lawton, C. L.; Blundell, J. E. Serotonergic drugs: effects on appetite expression and use for the treatment of obesity. *Drugs* **2007**, *67*, 27−55.

(10) Kroeze, W. K.; Kristiansen, K.; Roth, B. L. Molecular biology of serotonin receptors structure and function at the molecular level. *Curr. Top. Med. Chem.* **2002**, *2*, 507−528.

(11) Hannon, J.; Hoyer, D. Molecular biology of 5-HT receptors. *Behav. Brain Res.* **2008**, *195*−*213*, 198.

(12) Millan, M. J.; Marin, P.; Bockaert, J.; la Cour, C. M. Signaling at G-protein-coupled serotonin receptors: recent advances and future research directions. *Trends Pharmacol. Sci.* **2008**, *29*, 454−464.

(13) Jensen, A. A.; Davies, P. A.; Bräuner-Osborne, H.; Krzywkowski, K. 3B but which 3B? And that's just one of the questions: the

heterogeneity of human 5-HT$_3$ receptors. *Trends Pharmacol. Sci.* **2008**, *29*, 437−444.
(14) Roth, B. L.; Willins, D. L.; Kristiansen, K.; Kroeze, W. K. 5-Hydroxytryptamine$_2$-family receptors (5-hydroxytryptamine$_{2A}$, 5-hydroxytryptamine$_{2B}$, 5-hydroxytryptamine$_{2C}$): where structure meets function. *Pharmacol. Ther.* **1998**, *79*, 231−257.
(15) Leysen, J. E. 5-HT$_2$ receptors. *CNS Neurol. Disord.: Drug Targets* **2004**, *3*, 11−26.
(16) Gonzalez-Maeso, J.; Sealfon, S. C. Psychedelics and schizophrenia. *Trends Neurosci.* **2009**, *32*, 225−232.
(17) Roth, B. L. Irving Page Lecture: 5-HT$_{2A}$ serotonin receptor biology: interacting proteins, kinases and paradoxical regulation. *Neuropharmacology* **2011**, *61*, 348−354.
(18) Brea, J.; Castro-Palomino, J.; Yeste, S.; Cubero, E.; Parraga, A.; Dominguez, E.; Loza, M. I. Emerging opportunities and concerns for drug discovery at serotonin 5-HT$_{2B}$ receptors. *Curr. Top. Med. Chem.* **2010**, *10*, 493−503.
(19) Hutcheson, J. D.; Setola, V.; Roth, B. L.; Merryman, W. D. Serotonin receptors and heart valve disease—it was meant 2B. *Pharmacol. Ther.* **2011**, *132*, 146−157.
(20) Clemett, D. A.; Punhani, T.; Duxon, M. S.; Blackburn, T. P.; Fone, K. C. Immunohistochemical localisation of the 5-HT$_{2C}$ receptor protein in the rat CNS. *Neuropharmacology* **2000**, *39*, 123−132.
(21) Serrats, J.; Mengod, G.; Cortes, R. Expression of serotonin 5-HT$_{2C}$ receptors in GABAergic cells of the anterior raphe nuclei. *J. Chem. Neuroanat.* **2005**, *29*, 83−91.
(22) Jensen, N. H.; Cremers, T. I.; Sotty, F. Therapeutic potential of 5-HT$_{2C}$ receptor ligands. *Sci.World J.* **2010**, *10*, 1870−1885.
(23) Wacker, D. A.; Miller, K. J. Agonists of the serotonin 5-HT$_{2C}$ receptor: preclinical and clinical progression in multiple diseases. *Curr. Opin. Drug Discovery Dev.* **2008**, *11*, 438−445.
(24) Millan, M. J. Serotonin 5-HT$_{2C}$ receptors as a target for the treatment of depressive and anxious states: focus on novel therapeutic strategies. *Therapie* **2005**, *60*, 441−460.
(25) Isaac, M. Serotonergic 5-HT$_{2C}$ receptors as a potential therapeutic target for the design antiepileptic drugs. *Curr. Top. Med. Chem.* **2005**, *5*, 59−67.
(26) Halford, J. C.; Harrold, J. A. 5-HT$_{2C}$ receptor agonists and the control of appetite. *Handb. Exp. Pharmacol.* **2012**, 349−356.
(27) Krogsgaard-Larsen, P.; Frølund, B.; Liljefors, T.; Ebert, B. GABA$_A$ agonists and partial agonists: THIP (Gaboxadol) as a non-opioid analgesic and a novel type of hypnotic. *Biochem. Pharmacol.* **2004**, *68*, 1573−1580.
(28) Krogsgaard-Larsen, P.; Hjeds, H. Organic hydroxylamine derivatives. X. Structural analogues of γ-aminobutyric acid (GABA) of the Isoxazole enol-betaine type. Synthesis of 5,6,7,8-tetrahydro-4*H*-isoxazolo[4,5-*d*]azepin-3-ol zwitterion and 4,5,6,7-tetrahydrisoxazolo-[4,5-*c*]pyridin-3-ol zwitterion. *Acta Chem. Scand.* **1974**, *B28*, 533−538.
(29) Krogsgaard-Larsen, P.; Hjeds, H.; Curtis, D. R.; Leah, J. D.; Peet, M. J. Glycine antagonists structurally related to muscimol, THIP, or isoguvacine. *J. Neurochem.* **1982**, *39*, 1319−1324.
(30) Krogsgaard-Larsen, P.; Mikkelsen, H.; Jacobsen, P.; Falch, E.; Curtis, D. R.; Peet, M. J.; Leah, J. D. 4,5,6,7-Tetrahydroisothiazolo[5,4-*c*]pyridin-3-ol and related analogues of THIP. Synthesis and biological activity. *J. Med. Chem.* **1983**, *26*, 895−900.
(31) Carniaux, J.-F.; Cummins, J. Compositions and methods of synthesis of pyridinoylpiperidine 5-HT$_{1F}$ agonists. WO/2011/123654 A1, 2011.
(32) Krogsgaard-Larsen, P. Muscimol Analogues. II Synthesis of Some Bicyclic 3-Isoxazolol Zwitterions. *Acta Chem. Scand.* **1977**, *B31*, 584−588.
(33) Schlag, B. D.; Lou, Z.; Fennell, M.; Dunlop, J. Ligand dependency of 5-hydroxytryptamine 2C receptor internalization. *J. Pharmacol. Exp. Ther.* **2004**, *310*, 865−870.
(34) Acuna-Castillo, C.; Villalobos, C.; Moya, P. R.; Saez, P.; Cassels, B. K.; Huidobro-Toro, J. P. Differences in potency and efficacy of a series of phenylisopropylamine/phenylethylamine pairs at 5-HT$_{2A}$ and 5-HT$_{2C}$ receptors. *Br. J. Pharmacol.* **2002**, *136*, 510−519.
(35) Smith, B. M.; Smith, J. M.; Tsai, J. H.; Schultz, J. A.; Gilson, C. A.; Estrada, S. A.; Chen, R. R.; Park, D. M.; Prieto, E. B.; Gallardo, C. S.; Sengupta, D.; Dosa, P. I.; Covel, J. A.; Ren, A.; Webb, R. R.; Beeley, N. R.; Martin, M.; Morgan, M.; Espitia, S.; Saldana, H. R.; Bjenning, C.; Whelan, K. T.; Grottick, A. J.; Menzaghi, F.; Thomsen, W. J. Discovery and structure−activity relationship of (1*R*)-8-chloro-2,3,4,5-tetrahydro-1-methyl-1*H*-3-benzazepine (Lorcaserin), a selective serotonin 5-HT$_{2C}$ receptor agonist for the treatment of obesity. *J. Med. Chem.* **2008**, *51*, 305−313.
(36) Siuciak, J. A.; Chapin, D. S.; McCarthy, S. A.; Guanowsky, V.; Brown, J.; Chiang, P.; Marala, R.; Patterson, T.; Seymour, P. A.; Swick, A.; Iredale, P. A. CP-809,101, a selective 5-HT$_{2C}$ agonist, shows activity in animal models of antipsychotic activity. *Neuropharmacology* **2007**, *52*, 279−290.
(37) Porter, R. H.; Benwell, K. R.; Lamb, H.; Malcolm, C. S.; Allen, N. H.; Revell, D. F.; Adams, D. R.; Sheardown, M. J. Functional characterization of agonists at recombinant human 5-HT$_{2A}$, 5-HT$_{2B}$, and 5-HT$_{2C}$ receptors in CHO-K1 cells. *Br. J. Pharmacol.* **1999**, *128*, 13−20.
(38) Jerman, J. C.; Brough, S. J.; Gager, T.; Wood, M.; Coldwell, M. C.; Smart, D.; Middlemiss, D. N. Pharmacological characterisation of human 5-HT$_2$ receptor subtypes. *Eur. J. Pharmacol.* **2001**, *414*, 23−30.
(39) Weiner, D. M.; Burstein, E. S.; Nash, N.; Croston, G. E.; Currier, E. A.; Vanover, K. E.; Harvey, S. C.; Donohue, E.; Hansen, H. C.; Andersson, C. M.; Spalding, T. A.; Gibson, D. F.; Krebs-Thomson, K.; Powell, S. B.; Geyer, M. A.; Hacksell, U.; Brann, M. R. 5-Hydroxytryptamine$_{2A}$ receptor inverse agonists as antipsychotics. *J. Pharmacol. Exp. Ther.* **2001**, *299*, 268−276.
(40) Shahid, M.; Walker, G. B.; Zorn, S. H.; Wong, E. H. Asenapine: a novel psychopharmacologic agent with a unique human receptor signature. *J. Psychopharmacol.* **2009**, *23*, 65−73.
(41) Aloyo, V. J.; Harvey, J. A. Antagonist binding at 5-HT$_{2A}$ and 5-HT$_{2C}$ receptors in the rabbit: high correlation with the profile for the human receptors. *Eur. J. Pharmacol.* **2000**, *406*, 163−169.
(42) Lameh, J.; McFarland, K.; Ohlsson, J.; Ek, F.; Piu, F.; Burstein, E. S.; Tabatabaei, A.; Olsson, R.; Bradley, S. R.; Bonhaus, D. W. Discovery of potential antipsychotic agents possessing pro-cognitive properties. *Naunyn Schmiedeberg's Arch. Pharmacol.* **2012**, *385*, 313−323.
(43) Thomsen, A. R. B.; Hvidtfeldt, M.; Bräuner-Osborne, H. Biased agonism of the calcium-sensing receptor. *Cell Calcium* **2012**, *51*, 107−116.
(44) Knight, A. R.; Misra, A.; Quirk, K.; Benwell, K.; Revell, D.; Kennett, G.; Bickerdike, M. Pharmacological characterisation of the agonist radioligand binding site of 5-HT$_{2A}$, 5-HT$_{2B}$ and 5-HT$_{2C}$ receptors. *Naunyn Schmiedeberg's Arch. Pharmacol.* **2004**, *370*, 114−123.
(45) Muntasir, H. A.; Takahashi, J.; Rashid, M.; Ahmed, M.; Komiyama, T.; Hossain, M.; Kawakami, J.; Nashimoto, M.; Nagatomo, T. Site-directed mutagenesis of the serotonin 5-hydroxytryptamine2c receptor: identification of amino acids responsible for sarpogrelate binding. *Biol. Pharm. Bull.* **2006**, *29*, 1645−1650.
(46) Xie, J.; Dernovici, S.; Ribeiro, P. Mutagenesis analysis of the serotonin 5-HT$_{2C}$ receptor and a *Caenorhabditis elegans* 5-HT$_2$ homologue: conserved residues of helix 4 and helix 7 contribute to agonist-dependent activation of 5-HT$_2$ receptors. *J. Neurochem.* **2005**, *92*, 375−387.
(47) Sleight, A. J.; Stam, N. J.; Mutel, V.; Vanderheyden, P. M. Radiolabelling of the human 5-HT$_{2A}$ receptor with an agonist, a partial agonist and an antagonist: effects on apparent agonist affinities. *Biochem. Pharmacol.* **1996**, *51*, 71−76.
(48) Rosenkilde, M. M.; Cahir, M.; Gether, U.; Hjorth, S. A.; Schwartz, T. W. Mutations along transmembrane segment II of the NK-1 receptor affect substance P competition with non-peptide antagonists but not substance P binding. *J. Biol. Chem.* **1994**, *269*, 28160−28164.
(49) Hjorth, S. A.; Thirstrup, K.; Schwartz, T. W. Radioligand-dependent discrepancy in agonist affinities enhanced by mutations in the kappa-opioid receptor. *Mol. Pharmacol.* **1996**, *50*, 977−984.
(50) Sagan, S.; Beaujouan, J. C.; Torrens, Y.; Saffroy, M.; Chassaing, G.; Glowinski, J.; Lavielle, S. High affinity binding of [3*H*]propionyl-[Met(O2)11]substance P(7−11), a tritiated septide-like peptide, in

Chinese hamster ovary cells expressing human neurokinin-1 receptors and in rat submandibular glands. *Mol. Pharmacol.* **1997**, *52*, 120−127.
(51) Rosenkilde, M. M.; Schwartz, T. W. Potency of ligands correlates with affinity measured against agonist and inverse agonists but not against neutral ligand in constitutively active chemokine receptor. *Mol. Pharmacol.* **2000**, *57*, 602−609.
(52) Isberg, V.; Balle, T.; Sander, T.; Jørgensen, F. S.; Gloriam, D. E. G protein- and agonist-bound serotonin 5-HT_{2A} receptor model activated by steered molecular dynamics simulations. *J. Chem. Inf. Model.* **2011**, *51*, 315−325.
(53) Ballosteros, J. A.; Weinstein, H. Integrated methods for the construction of three dimensional models and computational probing of structure function relations in G protein-coupled receptors. In *Methods in Neurosciences*; Sealfon, S. C., Conn, P. M., Eds.; Academic Press: San Diego, CA, 1995; Vol. *25*, pp 366−428.
(54) Meltzer, H. Y.; Nash, J. F. Effects of antipsychotic drugs on serotonin receptors. *Pharmacol. Rev.* **1991**, *43*, 587−604.
(55) Martin, G. E.; Elgin, R. J., Jr.; Mathiasen, J. R.; Davis, C. B.; Kesslick, J. M.; Baldy, W. J.; Shank, R. P.; DiStefano, D. L.; Fedde, C. L.; Scott, M. K. Activity of aromatic substituted phenylpiperazines lacking affinity for dopamine binding sites in a preclinical test of antipsychotic efficacy. *J. Med. Chem.* **1989**, *32*, 1052−1056.
(56) Martin, G. E.; Elgin, R. J., Jr.; Kesslick, J. M.; Baldy, W. J.; Mathiasen, J. R.; Shank, R. P.; Scott, M. K. Block of conditioned avoidance responding in the rat by substituted phenylpiperazines. *Eur. J. Pharmacol.* **1988**, *156*, 223−229.
(57) Meltzer, H. Y.; Massey, B. W.; Horiguchi, M. Serotonin receptors as targets for drugs useful to treat psychosis and cognitive impairment in schizophrenia. *Curr. Pharm. Biotechnol.* **2012**, *13*, 1572−1586.
(58) Brennan, P. E.; Whitlock, G. A.; Ho, D. K.; Conlon, K.; McMurray, G. Discovery of a novel azepine series of potent and selective 5-HT_{2C} agonists as potential treatments for urinary incontinence. *Bioorg. Med. Chem. Lett.* **2009**, *19*, 4999−5003.
(59) Nichols, D. E. Structure−activity relationships of serotonin 5-HT_{2A} agonists. *WIREs: Membr. Transp. Signaling* **2012**, DOI: 10.1002/wmts.42.
(60) Trachsel, D.; Nichols, D. E.; Kidd, S.; Hadorn, M.; Baumberger, F. 4-Aryl-substituted 2,5-dimethoxyphenethylamines: synthesis and serotonin 5-HT_{2A} receptor affinities. *Chem Biodiversity* **2009**, *6*, 692−704.
(61) Nichols, D. E. Hallucinogens. *Pharmacol. Ther.* **2004**, *101*, 131−181.
(62) Sellin, A. K.; Shad, M.; Tamminga, C. Muscarinic agonists for the treatment of cognition in schizophrenia. *CNS Spectrosc.* **2008**, *13*, 985−996.
(63) Dellu, F.; Mayo, W.; Cherkaoui, J.; Le Moal, M.; Simon, H. A two-trial memory task with automated recording: study in young and aged rats. *Brain Res.* **1992**, *588*, 132−139.
(64) Calcagno, E.; Carli, M.; Baviera, M.; Invernizzi, R. W. Endogenous serotonin and serotonin$_{2C}$ receptors are involved in the ability of M100907 to suppress cortical glutamate release induced by NMDA receptor blockade. *J. Neurochem.* **2009**, *108*, 521−532.
(65) Marquis, K. L.; Sabb, A. L.; Logue, S. F.; Brennan, J. A.; Piesla, M. J.; Comery, T. A.; Grauer, S. M.; Ashby, C. R., Jr.; Nguyen, H. Q.; Dawson, L. A.; Barrett, J. E.; Stack, G.; Meltzer, H. Y.; Harrison, B. L.; Rosenzweig-Lipson, S. WAY-163909 [(7b*R*,10a**R**)-1,2,3,4,8,9,10,10a-Octahydro-7b*H*-cyclopenta-[*b*][1,4]diazepino[6,7,1*hi*]indole]: a novel 5-hydroxytryptamine 2C receptor-selective agonist with preclinical antipsychotic-like activity. *J. Pharmacol. Exp. Ther.* **2007**, *320*, 486−496.
(66) Landolt, H. P.; Wehrle, R. Antagonism of serotonergic 5-HT2A/2C receptors: mutual improvement of sleep, cognition and mood? *Eur. J. Neurosci.* **2009**, *29*, 1795−1809.
(67) Frydenvang, K.; Pickering, D. S.; Greenwood, J. R.; Krogsgaard-Larsen, N.; Brehm, L.; Nielsen, B.; Vogensen, S. B.; Hald, H.; Kastrup, J. S.; Krogsgaard-Larsen, P.; Clausen, R. P. Biostructural and Pharmacological Studies of Bicyclic Analogues of the 3-Isoxazolol Glutamate Receptor Agonist Ibotenic Acid. *J. Med. Chem.* **2010**, *53*, 8354−8361.
(68) Høg, S.; Greenwood, J. R.; Madsen, K. B.; Larsson, O. M.; Frølund, B.; Schousboe, A.; Krogsgaard-Larsen, P.; Clausen, R. P. Structure−activity relationships of selective GABA uptake inhibitors. *Curr. Top. Med. Chem.* **2006**, *6*, 1861−1882.
(69) Gottlieb, H. E.; Kotlyar, V.; Nudelman, A. NMR Chemical Shifts of Common Laboratory Solvents as Trace Impurities. *J. Org. Chem.* **1997**, *62*, 7512−7515.
(70) Jensen, A. A.; Christesen, T.; Bølcho, U.; Greenwood, J. R.; Postorino, G.; Vogensen, S. B.; Johansen, T. N.; Egebjerg, J.; Bräuner-Osborne, H.; Clausen, R. P. Functional characterization of Tet-AMPA [tetrazolyl-2-amino-3-(3-hydroxy-5-methyl- 4-isoxazolyl)propionic acid] analogues at ionotropic glutamate receptors GluR1-GluR4. The molecular basis for the functional selectivity profile of 2-Bn-Tet-AMPA. *J. Med. Chem.* **2007**, *50*, 4177−4185.
(71) Trattnig, S. M.; Harpsøe, K.; Thygesen, S. B.; Rahr, L. M.; Ahring, P. K.; Balle, T.; Jensen, A. A. Discovery of a novel allosteric modulator of 5-HT_3 receptors: inhibition and potentiation of Cys-loop receptor signaling through a conserved transmembrane intersubunit site. *J. Biol. Chem.* **2012**, *287*, 25241−25254.
(72) Krogsgaard-Larsen, N.; Jensen, A. A.; Kehler, J. Novel 7-phenylsulfanyl-1,2,3,4,10,10a-hexahydro-pyrazino[1,2-*a*]indoles as dual serotonin 5-HT_{2C} and 5-HT_6 receptor ligands. *Bioorg. Med. Chem. Lett.* **2010**, *20*, 5431−5433.
(73) Ransom, R. W.; Stec, N. L. Cooperative modulation of [^{3}H]MK-801 binding to the *N*-methyl-D-aspartate receptor-ion channel complex by L-glutamate, glycine, and polyamines. *J. Neurochem.* **1988**, *51*, 830−836.
(74) Paxinos, G.; Watson, C. *The Rat Brain in Stereotaxic Coordinates*. 4th ed.; Academic Press: San Diego, 1998.
(75) Wellendorph, P.; Høg, S.; Sabbatini, P.; Pedersen, M. H.; Martiny, L.; Knudsen, G. M.; Frølund, B.; Clausen, R. P.; Bräuner-Osborne, H. Novel radioiodinated γ-hydroxybutyric acid analogues for radiolabeling and photolinking of high-affinity γ-hydroxybutyric acid binding sites. *J. Pharmacol. Exp. Ther.* **2010**, *335*, 458−464.
(76) Dellu, F.; Fauchey, V.; Le Moal, M.; Simon, H. Extension of a new two-trial memory task in the rat: influence of environmental context on recognition processes. *Neurobiol. Learn. Mem.* **1997**, *67*, 112−120.
(77) Dellu, F.; Mayo, W.; Vallee, M.; Le Moal, M.; Simon, H. Facilitation of cognitive performance in aged rats by past experience depends on the type of information processing involved: a combined cross-sectional and longitudinal study. *Neurobiol. Learn. Mem.* **1997**, *67*, 121−128.
(78) Friesner, R. A.; Banks, J. L.; Murphy, R. B.; Halgren, T. A.; Klicic, J. J.; Mainz, D. T.; Repasky, M. P.; Knoll, E. H.; Shelley, M.; Perry, J. K.; Shaw, D. E.; Francis, P.; Shenkin, P. S. Glide: a new approach for rapid, accurate docking and scoring. 1. Method and assessment of docking accuracy. *J. Med. Chem.* **2004**, *47*, 1739−1749.